Bode Diagrams of Transfer Functions and Impedances

ECEN 2260 Supplementary Notes
R. W. Erickson

In the design of a signal processing network, control system, or other analog system, it is usually necessary to work with frequency-dependent transfer functions and impedances, and to construct Bode diagrams. The Bode diagram is a log-log plot of the magnitude and phase of an impedance, transfer function, or other frequency-dependent complex-valued quantity, as a function of the frequency of a sinusoidal excitation. The objective of this handout is to describe the basic rules for constructing Bode diagrams, to illustrate some useful approximations, and to develop some physical insight into the frequency response of linear circuits. Experimental measurement of transfer functions and impedances is briefly discussed.

Real systems are complicated, and hence their analysis often leads to complicated derivations, long equations, and lots of algebra mistakes. And the long equations are not useful for design unless they can be inverted, so that the engineer can choose element values to obtain a given desired behavior. It is further desired that the engineer gain insight sufficient to design the system, often including synthesizing a new circuit, adding elements to an existing circuit, changing connections in an existing circuit, or changing existing element values. So *design-oriented analysis* is needed [1]. Some tools for approaching the design of a complicated converter system are described in these notes. Writing the transfer functions in normalized form directly exposes the important features of the response. Analytical expressions for these features, as well as for the asymptotes, lead to simple equations that are useful in design. Well-separated roots of transfer function polynomials can be approximated in a simple way. Section 3 describes a graphical method for constructing Bode plots of transfer functions and impedances, essentially by inspection. If you can do this, then: (1) it's less work and less algebra, with fewer algebra mistakes; (2) you have much greater insight into circuit behavior, which can be applied to design the circuit; (3) approximations become obvious.

1. Bode plots: basic rules

A Bode plot is a plot of the magnitude and phase of a transfer function or other complex-valued quantity, versus frequency. Magnitude in decibels, and phase in degrees, are plotted vs. frequency, using semi-logarithmic axes. The magnitude plot is effectively a log-log plot, since the magnitude is expressed in decibels and the frequency axis is logarithmic.

The magnitude of a dimensionless quantity G can be expressed in decibels as follows:

$$\| G \|_{\text{dB}} = 20 \log_{10}\left(\| G \| \right) \tag{1}$$

Decibel values of some simple magnitudes are listed in Table 1. Care must be used when the magnitude is not dimensionless. Since it is not proper to take the logarithm of a quantity having dimensions, the magnitude must first be normalized. For example, to express the magnitude of an impedance Z in decibels, we should normalize by dividing by a base impedance R_{base}:

Table 1. Expressing magnitudes in decibels

Actual magnitude	*Magnitude in dB*
1/2	– 6dB
1	0 dB
2	6 dB
5 = 10/2	20 dB – 6 dB = 14 dB
10	20dB
$1000 = 10^3$	3 · 20dB = 60 dB

$$\| Z \|_{\text{dB}} = 20 \log_{10}\left(\frac{\| Z \|}{R_{base}} \right) \tag{2}$$

The value of R_{base} is arbitrary, but we need to tell others what value we have used. So if $\| Z \|$ is 5Ω, and we choose R_{base} = 10Ω, then we can say that $\| Z \|_{\text{dB}}$ = 20 $\log_{10}$(5Ω/10Ω) = – 6dB with respect to 10Ω. A common choice is R_{base} = 1Ω; decibel impedances expressed with R_{base} = 1Ω are said to be expressed in dBΩ. So 5Ω is equivalent to 14dBΩ. Current switching harmonics at the input port of a converter are often expressed in dBμA, or dB using a base current of 1μA: 60dBμA is equivalent to 1000μA, or 1mA.

The magnitude Bode plots of functions equal to powers of f are linear. For example, suppose that the magnitude of a dimensionless quantity $G(f)$ is

$$\| G \| = \left(\frac{f}{f_0} \right)^n \tag{3}$$

where f_0 and n are constants. The magnitude in decibels is

$$\| G \|_{\text{dB}} = 20 \log_{10}\left(\frac{f}{f_0} \right)^n = 20n \log_{10}\left(\frac{f}{f_0} \right) \tag{4}$$

This equation is plotted in Fig. 1, for several values of n. The magnitudes have value 1 ⇒ 0dB at frequency $f = f_0$. They are linear functions of $\log_{10}(f)$. The slope is the change in $\| G \|_{\text{dB}}$ arising from a unit change in $\log_{10}(f)$; a unit increase in $\log_{10}(f)$ corresponds to a factor of 10, or decade, increase in f. From Eq. (4), a decade increase in f leads to an increase in $\| G \|_{\text{dB}}$ of $20n$ dB. Hence, the slope is $20n$ dB per decade. Equivalently, we can say that the slope is $20n \log_{10}(2) \approx 6n$ dB per octave, where an octave is a factor of 2 change in frequency. In practice, the magnitudes of most frequency-dependent functions can usually be approximated over a limited range of frequencies by functions of the form (3); over this range of frequencies, the magnitude Bode plot is approximately linear with slope $20n$ dB/decade.

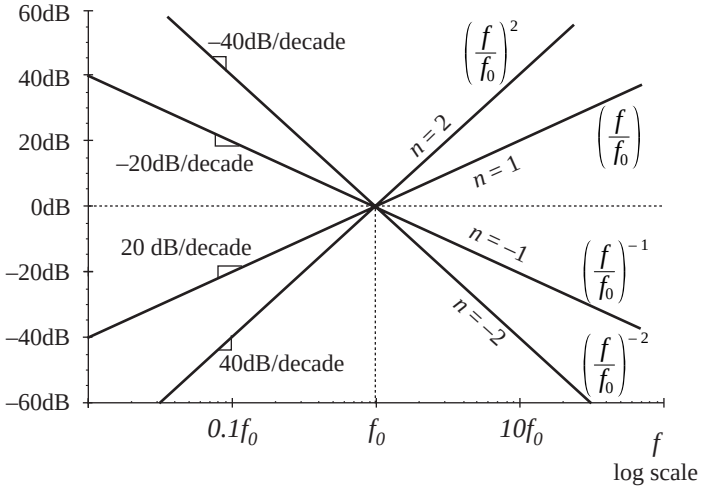

Fig. 1. Magnitude Bode plots of functions which vary as f^n are linear, with slope n dB per decade.

1.1. Single pole response

Consider the simple *R*-*C* low-pass filter illustrated in Fig. 2. The transfer function is given by the voltage divider ratio

$$G(s) = \frac{v_2(s)}{v_1(s)} = \frac{\frac{1}{sC}}{\frac{1}{sC} + R} \qquad (5)$$

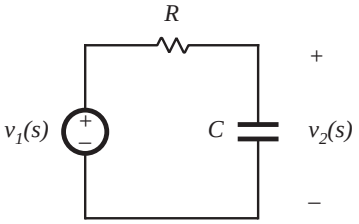

Fig. 2. Simple *R*-*C* low-pass filter example.

This transfer function is a ratio of voltages, and hence is dimensionless. By multiplying the numerator and denominator by sC, we can express the transfer function as a rational fraction:

$$G(s) = \frac{1}{1 + sRC} \qquad (6)$$

The transfer function now coincides with the following standard normalized form for a single pole:

$$G(s) = \frac{1}{\left(1 + \frac{s}{\omega_0}\right)} \qquad (7)$$

The parameter $\omega_0 = 2\pi f_0$ is found by equating the coefficients of s in the denominators of Eqs. (6) and (7). The result is

$$\omega_0 = \frac{1}{RC} \tag{8}$$

Since R and C are real positive quantities, ω_0 is also real and positive. The denominator of Eq. (7) contains a root at $s = -\omega_0$, and hence $G(s)$ contains a real pole in the left half of the complex plane.

To find the magnitude and phase of the transfer function, we let $s = j\omega$, where j is the square root of -1. We then find the magnitude and phase of the resulting complex-valued function. With $s = j\omega$, Eq. (7) becomes

$$G(j\omega) = \frac{1}{\left(1 + j\,\frac{\omega}{\omega_0}\right)} = \frac{1 - j\,\frac{\omega}{\omega_0}}{1 + \left(\frac{\omega}{\omega_0}\right)^2} \tag{9}$$

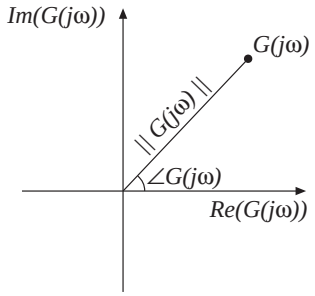

Fig. 3. Magnitude and phase of the complex-valued function $G(j\omega)$.

The complex-valued $G(j\omega)$ is illustrated in Fig. 3, for one value of ω. The magnitude is

$$\left\| G(j\omega) \right\| = \sqrt{\left[\mathrm{Re}\,(G(j\omega))\right]^2 + \left[\mathrm{Im}\,(G(j\omega))\right]^2} = \frac{1}{\sqrt{1 + \left(\frac{\omega}{\omega_0}\right)^2}} \tag{10}$$

Here, we have assumed that ω_0 is real. In decibels, the magnitude is

$$\left\| G(j\omega) \right\|_{\mathrm{dB}} = -20 \log_{10} \left(\sqrt{1 + \left(\frac{\omega}{\omega_0}\right)^2} \right) \ \mathrm{dB} \tag{11}$$

The easy way to sketch the magnitude Bode plot of G is to investigate the asymptotic behavior for large and small frequency.

For small frequency, $\omega << \omega_0$ and $f << f_0$, it is true that

$$\left(\frac{\omega}{\omega_0}\right) << 1 \tag{12}$$

The $(\omega/\omega_0)^2$ term of Eq. (10) is therefore much smaller than 1, and hence Eq. (10) becomes

$$\left\| G(j\omega) \right\| \approx \frac{1}{\sqrt{1}} = 1 \tag{13}$$

In decibels, the magnitude is approximately

$$\left\| G(j\omega) \right\|_{\mathrm{dB}} \approx 0\mathrm{dB} \tag{14}$$

Thus, as illustrated in Fig. 4, at low frequency $\| G(j\omega) \|_{\mathrm{dB}}$ is asymptotic to 0dB.

At high frequency, $\omega >> \omega_0$ and $f >> f_0$. In this case, it is true that

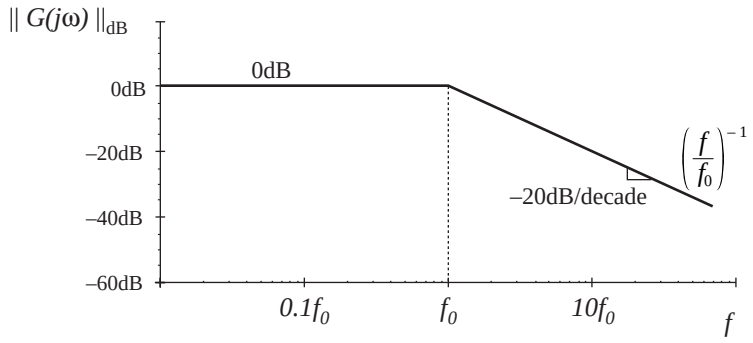

Fig. 4. Magnitude asymptotes for the single real pole transfer function.

$$\left(\frac{\omega}{\omega_0}\right) >> 1 \tag{15}$$

We can then say that

$$1 + \left(\frac{\omega}{\omega_0}\right)^2 \approx \left(\frac{\omega}{\omega_0}\right)^2 \tag{16}$$

Hence, Eq. (10) now becomes

$$\left\| G(j\omega) \right\| \approx \frac{1}{\sqrt{\left(\frac{\omega}{\omega_0}\right)^2}} = \left(\frac{f}{f_0}\right)^{-1} \tag{17}$$

This expression coincides with Eq. (3), with $n = -1$. So at high frequency, $\| G(j\omega) \|_{dB}$ has slope – 20dB per decade, as illustrated in Fig. 4. Thus, the asymptotes of $\| G(j\omega) \|$ are equal to 1 at low frequency, and $(f / f_0)^{-1}$ at high frequency. The asymptotes intersect at f_0. The actual magnitude tends towards these asymptotes at very low frequency and very high frequency. In the vicinity of the corner frequency f_0, the actual curve deviates somewhat from the asymptotes.

The deviation of the exact curve from the asymptotes can be found by simply evaluating Eq. (10). At the corner frequency $f = f_0$, Eq. (10) becomes

$$\left\| G(j\omega_0) \right\| = \frac{1}{\sqrt{1 + \left(\frac{\omega_0}{\omega_0}\right)^2}} = \frac{1}{\sqrt{2}} \tag{18}$$

In decibels, the magnitude is

$$\left\| G(j\omega_0) \right\|_{dB} = -20 \log_{10} \left(\sqrt{1 + \left(\frac{\omega_0}{\omega_0}\right)^2} \right) \approx -3 \text{ dB} \tag{19}$$

So the actual curve deviates from the asymptotes by –3dB at the corner frequency, as illustrated in Fig. 5. Similar arguments show that the actual curve deviates from the asymptotes by –1dB at $f = f_0/2$ and at $f = 2f_0$.

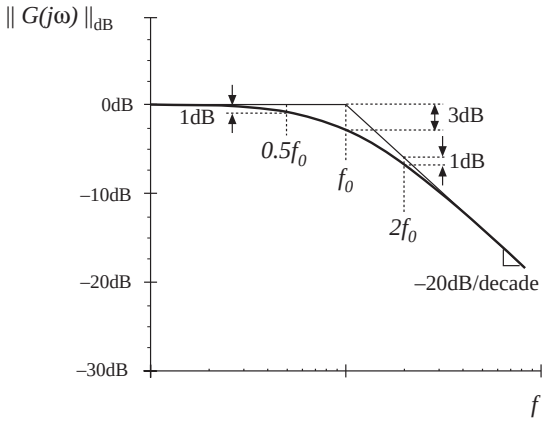

Fig. 5. Deviation of the actual curve from the asymptotes, for the transfer functions of the single real pole.

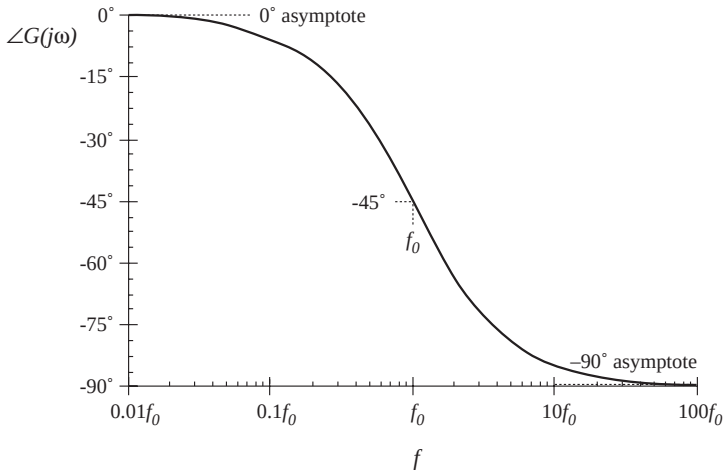

Fig. 6. Exact phase plot, single real pole.

The phase of $G(j\omega)$ is

$$\angle G(j\omega) = \tan^{-1}\left(\frac{\mathrm{Im}\left(G(j\omega)\right)}{\mathrm{Re}\left(G(j\omega)\right)}\right) \tag{20}$$

Insertion of the real and imaginary parts of Eq. (9) into Eq. (20) leads to

$$\angle G(j\omega) = -\tan^{-1}\left(\frac{\omega}{\omega_0}\right) \tag{21}$$

This function is plotted in Fig. 6. It tends to 0° at low frequency, and to –90° at high frequency. At the corner frequency $f = f_0$, the phase is –45°.

Since the high-frequency and low-frequency phase asymptotes do not intersect, we need a third asymptote to approximate the phase in the vicinity of the corner frequency f_0. One way to do this is illustrated in Fig. 7, where the slope of the asymptote is chosen to be identical to the slope of the actual curve at $f = f_0$. It can be shown that, with this choice, the asymptote intersection frequencies f_a and f_b are given by

$$\begin{aligned} f_a &= f_0\, e^{-\pi/2} \approx f_0 / 4.81 \\ f_b &= f_0\, e^{\pi/2} \approx 4.81\ f_0 \end{aligned} \tag{22}$$

A simpler choice, which better approximates the actual curve, is

$$\begin{aligned} f_a &= f_0 / 10 \\ f_b &= 10\ f_0 \end{aligned} \tag{23}$$

This asymptote is compared to the actual curve in Fig. 8. The pole causes the phase to change over a frequency span of approximately two decades, centered at the corner frequency. The slope of the asymptote in this frequency span is –45˚ per decade. At the break frequencies f_a and f_b, the actual phase deviates from the asymptotes by $\tan^{-1}(0.1) = 5.7^\circ$.

The magnitude and phase asymptotes for the single-pole response are summarized in Fig. 9.

It is good practice to consistently express single-pole transfer functions in the normalized form of Eq. (7). Both terms in the denominator of Eq. (7) are dimensionless, and the coefficient of s^0 is unity. Equation (7) is easy to interpret, because of its normalized form. At low frequencies, where the (s/ω_0) term is small in magnitude, the transfer function is approximately equal to 1. At high frequencies, where the (s/ω_0) term has magnitude much greater than 1, the transfer function is approximately

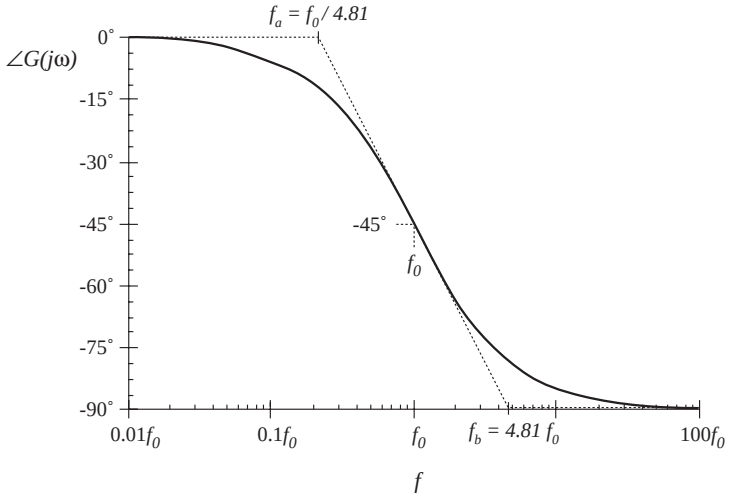

Fig. 7. One choice for the midfrequency phase asymptote, which correctly predicts the actual slope at $f = f_0$.

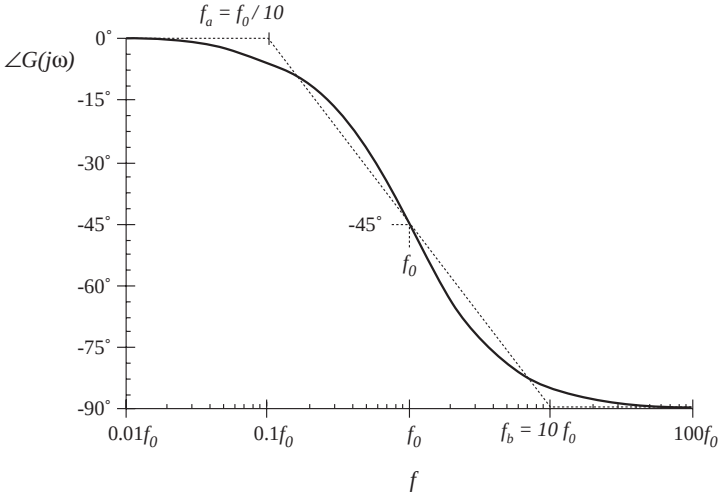

Fig. 8. A simpler choice for the midfrequency phase asymptote, which better approximates the curve over the entire frequency range.

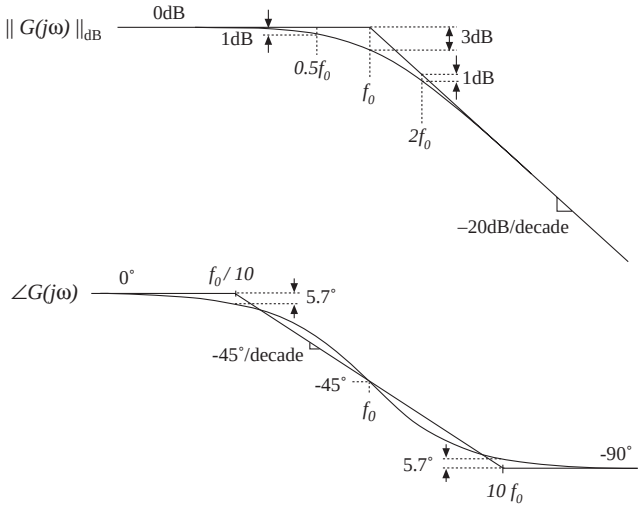

Fig. 9. Summary of the magnitude and phase Bode plot for the single real pole.

$(s/\omega_0)^{-1}$. This leads to a magnitude of $(f/f_0)^{-1}$. The corner frequency is $f_0 = \omega_0/2\pi$. So the transfer function is written directly in terms of its salient features, i.e., its asymptotes and its corner frequency.

1.2. Single zero response

A single zero response contains a root in the numerator of the transfer function, and can be written in the following normalized form:

$$G(s) = \left(1 + \frac{s}{\omega_0}\right) \tag{24}$$

This transfer function has magnitude

$$\left\| G(j\omega) \right\| = \sqrt{1 + \left(\frac{\omega}{\omega_0}\right)^2} \tag{25}$$

At low frequency, $f << f_0 = \omega_0/2\pi$, the transfer function magnitude tends to $1 \Rightarrow 0$dB. At high frequency, $f >> f_0$, the transfer function magnitude tends to (f/f_0). As illustrated in Fig. 10, the high frequency asymptote has slope +20dB/decade.

The phase is given by

$$\angle G(j\omega) = \tan^{-1}\left(\frac{\omega}{\omega_0}\right) \tag{26}$$

With the exception of a minus sign, the phase is identical to Eq. (21). Hence, suitable asymptotes are as illustrated in Fig. 10. The phase tends to 0˚ at low frequency, and to +90˚ at high frequency. Over the interval $f_0/10 < f < 10f_0$, the phase asymptote has a slope of +45˚/decade.

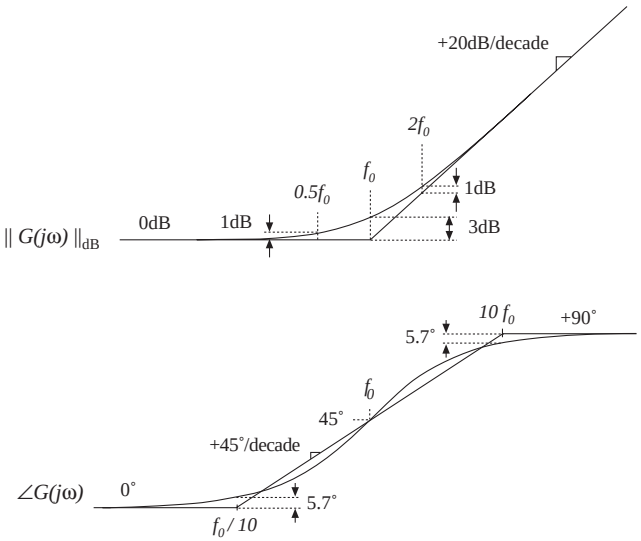

Fig. 10. Summary of the magnitude and phase Bode plot for the single real zero.

1.3. Frequency inversion

Two other forms arise, from inversion of the frequency axis. The inverted pole has the transfer function

$$G(s) = \frac{1}{\left(1 + \frac{\omega_0}{s}\right)} \qquad (27)$$

As illustrated in Fig. 11, the inverted pole has a high-frequency gain of 1, and a low frequency asymptote having a +20dB/decade slope. This form is useful for describing the gain of high-pass filters, and of other transfer functions where it is desired to emphasize the high frequency gain, with attenuation of low frequencies. Equation (27) is equivalent to

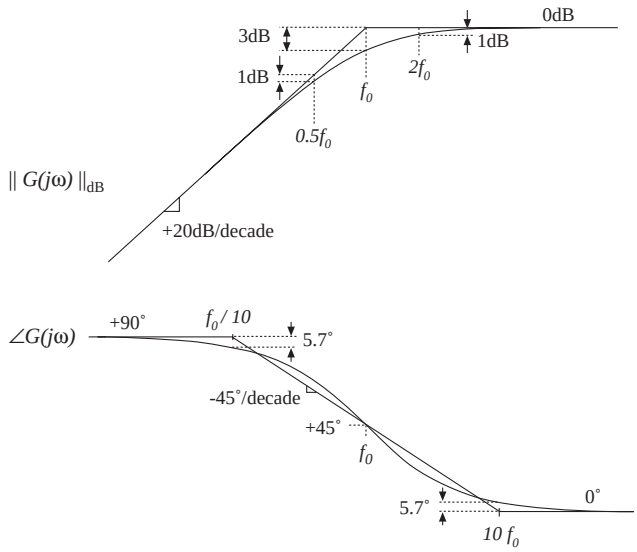

Fig. 11. Inversion of the frequency axis: summary of the magnitude and phase Bode plot for the inverted real pole.

$$G(s) = \frac{\left(\frac{s}{\omega_0}\right)}{\left(1 + \frac{s}{\omega_0}\right)} \qquad (28)$$

However, Eq. (27) more directly emphasizes that the high frequency gain is 1.

The inverted zero has the form

$$G(s) = \left(1 + \frac{\omega_0}{s}\right) \qquad (29)$$

As illustrated in Fig. 12, the inverted zero has a high-frequency gain asymptote equal to 1, and a low-frequency asymptote having a slope equal to –20dB/decade. An example of the use of this type of transfer function is the proportional-plus-integral controller, discussed in connection with feedback loop design in the next chapter. Equation (29) is equivalent to

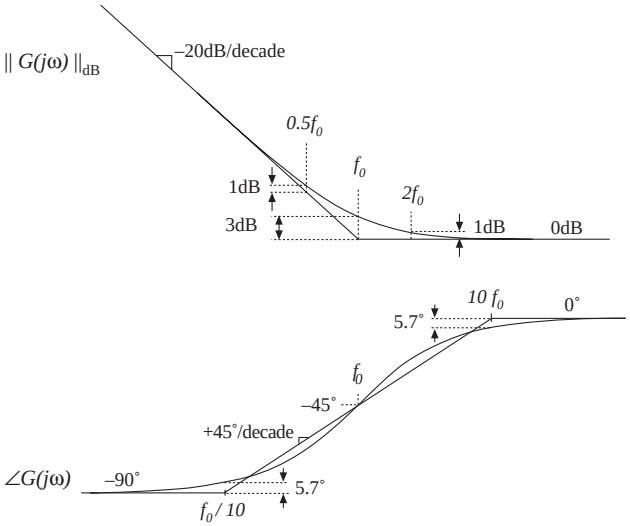

Fig. 12. Inversion of the frequency axis: summary of the magnitude and phase Bode plot for the inverted real zero.

$$G(s) = \frac{\left(1 + \frac{s}{\omega_0}\right)}{\left(\frac{s}{\omega_0}\right)} \tag{30}$$

However, Eq. (29) is the preferred form when it is desired to emphasize the value of the high-frequency gain asymptote.

The use of frequency inversion is illustrated by example in the next section.

1.4. Combinations

The Bode diagram of a transfer function containing several pole, zero, and gain terms, can be constructed by simple addition. At any given frequency, the magnitude (in decibels) of the composite transfer function is equal to the sum of the decibel magnitudes of the individual terms. Likewise, at a given frequency the phase of the composite transfer function is equal to the sum of the phases of the individual terms.

For example, suppose that we have already constructed the Bode diagrams of two complex-valued functions of ω, $G_1(\omega)$ and $G_2(\omega)$. These functions have magnitudes $R_1(\omega)$ and $R_2(\omega)$, and phases $\theta_1(\omega)$ and $\theta_2(\omega)$, respectively. It is desired to construct the Bode diagram of the product $G_3(\omega) = G_1(\omega)\, G_2(\omega)$. Let $G_3(\omega)$ have magnitude $R_3(\omega)$, and phase $\theta_3(\omega)$. To find this magnitude and phase, we can express $G_1(\omega)$, $G_2(\omega)$, and $G_3(\omega)$ in polar form:

$$\begin{aligned} G_1(\omega) &= R_1(\omega)\, e^{j\theta_1(\omega)} \\ G_2(\omega) &= R_2(\omega)\, e^{j\theta_2(\omega)} \\ G_3(\omega) &= R_3(\omega)\, e^{j\theta_3(\omega)} \end{aligned} \tag{31}$$

The product $G_3(\omega)$ can then be expressed as

$$G_3(\omega) = G_1(\omega)\, G_2(\omega) = R_1(\omega)\, e^{j\theta_1(\omega)}\, R_2(\omega)\, e^{j\theta_2(\omega)} \tag{32}$$

Simplification leads to

$$G_3(\omega) = \left(R_1(\omega)\, R_2(\omega)\right) e^{j(\theta_1(\omega) + \theta_2(\omega))} \tag{33}$$

Hence, the composite phase is

$$\theta_3(\omega) = \theta_1(\omega) + \theta_2(\omega) \tag{34}$$

The total magnitude is

$$R_3(\omega) = R_1(\omega)\, R_2(\omega) \tag{35}$$

When expressed in decibels, Eq. (35) becomes

$$\left| R_3(\omega) \right|_{\text{dB}} = \left| R_1(\omega) \right|_{\text{dB}} + \left| R_2(\omega) \right|_{\text{dB}} \tag{36}$$

So the composite phase is the sum of the individual phases, and when expressed in decibels, the composite magnitude is the sum of the individual magnitudes. The composite magnitude slope, in dB per decade, is therefore also the sum of the individual slopes in dB per decade.

For example, consider construction of the Bode plot of the following transfer function:

$$G(s) = \frac{G_0}{\left(1 + \frac{s}{\omega_1}\right)\left(1 + \frac{s}{\omega_2}\right)} \tag{37}$$

where $G_0 = 40 \Rightarrow 32\text{dB}$, $f_1 = \omega_1/2\pi = 100\text{Hz}$, $f_2 = \omega_2/2\pi = 2\text{kHz}$. This transfer function contains three terms: the gain G_0, and the poles at frequencies f_1 and f_2. The asymptotes for each of these terms are illustrated in Fig. 13. The gain G_0 is a positive real number, and therefore contributes zero phase shift with the gain 32dB. The poles at 100Hz and 2kHz each contribute asymptotes as in Fig. 9.

At frequencies less than 100Hz, the G_0 term contributes a gain magnitude of 32dB, while the two poles each contribute magnitude asymptotes of 0dB. So the low-frequency composite magnitude asymptote is 32dB + 0dB + 0dB = 32dB. For frequencies between 100Hz and 2kHz, the G_0 gain again contributes 32dB, and the pole at 2kHz continues to contribute a 0dB magnitude asymptote. However, the pole at 100Hz now contributes a magnitude asymptote that decreases with a –20dB/decade slope. The composite magnitude asymptote therefore also decreases with a –20dB/decade slope, as illustrated in Fig. 13. For frequencies greater than 2kHz, the poles at 100Hz and 2kHz each contribute decreasing

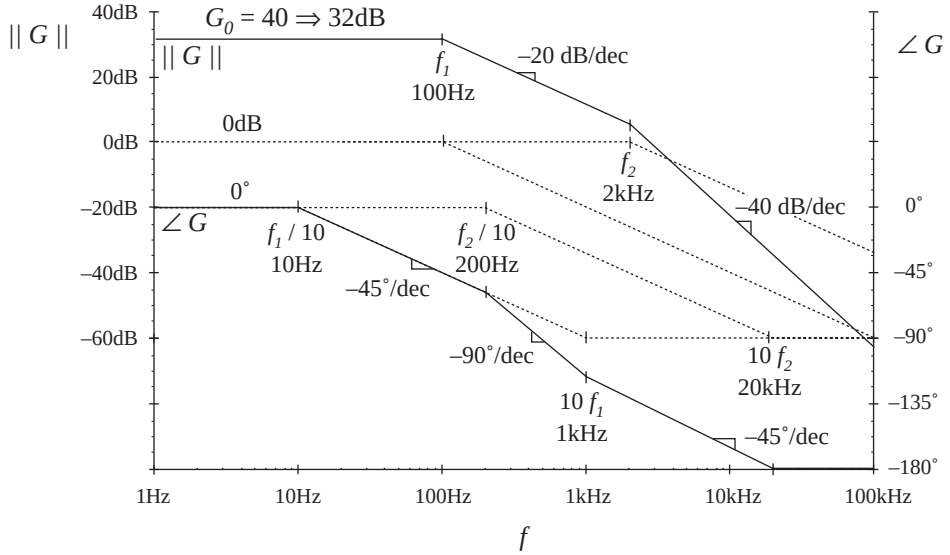

Fig. 13. Construction of magnitude and phase asymptotes for the transfer function of Eq. (37). Dashed lines: asymptotes for individual terms. Solid lines: composite asymptotes.

asymptotes having slopes of –20dB/decade. The composite asymptote therefore decreases with a slope of –20dB/decade –20dB/decade = –40dB/decade, as illustrated.

The composite phase asymptote is also constructed in Fig. 13. Below 10Hz, all terms contribute 0˚ asymptotes. For frequencies between $f_1/10$ = 10Hz, and $f_2/10$ = 200Hz, the pole at f_1 contributes a decreasing phase asymptote having a slope of –45˚/decade. Between 200Hz and $10f_1$ = 1kHz, both poles contribute decreasing asymptotes with–45˚/decade slopes; the composite slope is therefore –90˚/decade. Between 1kHz and $10f_2$ = 20kHz, the pole at f_1 contributes a constant –90˚ phase asymptote, while the pole at f_2 contributes a decreasing asymptote with –45˚/decade slope. The composite slope is then–45˚/decade. For frequencies greater than 20kHz, both poles contribute constant –90˚ asymptotes, leading to a composite phase asymptote of –180˚.

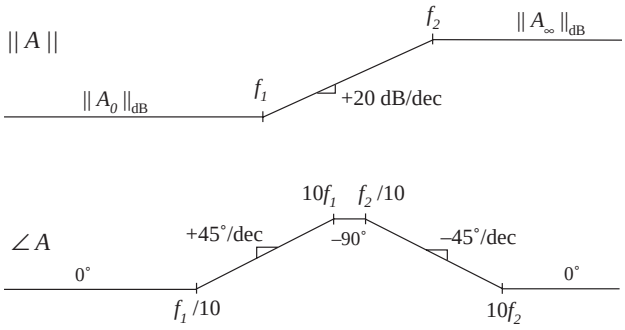

Fig. 14. Magnitude and phase asymptotes of example transfer function *A(s)*.

As a second example, consider the transfer function *A(s)* represented by the magnitude and phase asymptotes of Fig. 14. Let us write the transfer function that corresponds to these asymptotes. The dc asymptote is A_0. At corner frequency f_1, the asymptote slope increases from 0dB/decade to +20dB/decade. Hence, there must be a zero at frequency f_1. At frequency f_2, the asymptote slope decreases from +20dB/decade to 0dB/decade. Therefore the transfer function contains a pole at frequency f_2. So we can express the transfer function as

$$A(s) = A_0 \frac{\left(1 + \frac{s}{\omega_1}\right)}{\left(1 + \frac{s}{\omega_2}\right)} \tag{38}$$

where ω_1 and ω_2 are equal to $2\pi f_1$ and $2\pi f_2$, respectively.

We can use Eq. (38) to derive analytical expressions for the asymptotes. For $f < f_1$, and letting $s = j\omega$, we can see that the (s/ω_1) and (s/ω_2) terms each have magnitude less than 1. The asymptote is derived by neglecting these terms. Hence, the low-frequency magnitude asymptote is

$$\left\| A_0 \frac{\left(1 + \frac{s}{\omega_1}\right)}{\left(1 + \frac{s}{\omega_2}\right)} \right\|_{s = j\omega} = A_0 \frac{1}{1} = A_0 \tag{39}$$

For $f_1 < f < f_2$, the numerator term (s/ω_1) has magnitude greater than 1, while the denominator term (s/ω_2) has magnitude less than 1. The asymptote is derived by neglecting the smaller terms:

$$\left\| A_0 \frac{\left(1 + \frac{s}{\omega_1}\right)}{\left(1 + \frac{s}{\omega_2}\right)} \right\|_{s = j\omega} = A_0 \frac{\left\| \frac{s}{\omega_1} \right\|_{s = j\omega}}{1} = A_0 \frac{\omega}{\omega_1} = A_0 \frac{f}{f_1} \tag{40}$$

This is the expression for the midfrequency magnitude asymptote of $A(s)$. For $f > f_2$, the (s/ω_1) and (s/ω_2) terms each have magnitude greater than 1. The expression for the high-frequency asymptote is therefore:

$$\left\| A_0 \frac{\left(1 + \frac{s}{\omega_1}\right)}{\left(1 + \frac{s}{\omega_2}\right)} \right\|_{s = j\omega} = A_0 \frac{\left\| \frac{s}{\omega_1} \right\|_{s = j\omega}}{\left\| \frac{s}{\omega_2} \right\|_{s = j\omega}} = A_0 \frac{\omega_2}{\omega_1} = A_0 \frac{f_2}{f_1} \tag{41}$$

We can conclude that the high-frequency gain is

$$A_\infty = A_0 \frac{f_2}{f_1} \tag{42}$$

Thus, we can derive analytical expressions for the asymptotes.

The transfer function $A(s)$ can also be written in a second form, using inverted poles and zeroes. Suppose that $A(s)$ represents the transfer function of a high frequency amplifier, whose dc gain is not important. We are then interested in expressing $A(s)$ directly in terms of the high-frequency gain A_∞. We can view the transfer function as having an inverted pole at frequency f_2, which introduces attenuation at frequencies less than f_2. In addition, there is an inverted zero at $f = f_1$. So $A(s)$ could also be written

$$A(s) = A_\infty \frac{\left(1 + \frac{\omega_1}{s}\right)}{\left(1 + \frac{\omega_2}{s}\right)} \tag{43}$$

It can be verified that Eqs. (43) and (38) are equivalent.

1.5. Double pole response: resonance

Consider next the transfer function $G(s)$ of the two-pole low-pass filter of Fig. 15. One can show that the transfer function of this network is

$$G(s) = \frac{v_2(s)}{v_1(s)} = \frac{1}{1 + s\frac{L}{R} + s^2 LC} \tag{44}$$

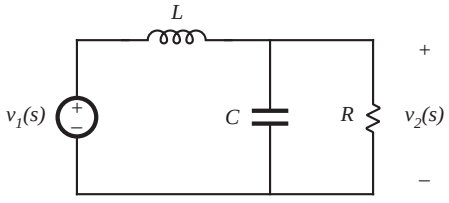

Fig. 15. Two-pole low-pass filter example.

This transfer function contains a second-order denominator polynomial, and is of the form

$$G(s) = \frac{1}{1 + a_1 s + a_2 s^2} \tag{45}$$

with $a_1 = L/R$ and $a_2 = LC$.

To construct the Bode plot of this transfer function, we might try to factor the denominator into its two roots:

$$G(s) = \frac{1}{\left(1 - \frac{s}{s_1}\right)\left(1 - \frac{s}{s_2}\right)} \tag{46}$$

Use of the quadratic formula leads to the following expressions for the roots:

$$s_1 = -\frac{a_1}{2a_2}\left[1 - \sqrt{1 - \frac{4a_2}{a_1^2}}\right] \tag{47}$$

$$s_2 = -\frac{a_1}{2a_2}\left[1 + \sqrt{1 - \frac{4a_2}{a_1^2}}\right] \tag{48}$$

If $4a_2 \leq a_1^2$, then the roots are real. Each real pole then exhibits a Bode diagram as derived in section 1.1, and the composite Bode diagram can be constructed as described in section 1.4 (but a better approach is described in section 1.6).

If $4a_2 > a_1^2$, then the roots (47) and (48) are complex. In section 1.1, the assumption was made that ω_0 is real; hence, the results of that section cannot be applied to this case. We need to do some additional work, to determine the magnitude and phase for the case when the roots are complex.

The transfer functions of Eqs. (44) and (45) can be written in the following standard normalized form:

$$G(s) = \frac{1}{1 + 2\zeta\frac{s}{\omega_0} + \left(\frac{s}{\omega_0}\right)^2} \tag{49}$$

If the coefficients a_1 and a_2 are real and positive, then the parameters ζ and ω_0 are also real and positive. The parameter ω_0 is again the angular corner frequency, and we can define $f_0 = \omega_0 / 2\pi$. The parameter ζ is called the *damping factor*: ζ controls the shape of the transfer function in the vicinity of $f = f_0$. An alternative standard normalized form is

$$G(s) = \frac{1}{1 + \frac{s}{Q\omega_0} + \left(\frac{s}{\omega_0}\right)^2} \tag{50}$$

where

$$Q = \frac{1}{2\zeta} \tag{51}$$

The parameter Q is called the quality factor of the circuit, and is a measure of the dissipation in the system. A more general definition of Q, for sinusoidal excitation of a passive element or network, is

$$Q = 2\pi \frac{\text{(peak stored energy)}}{\text{(energy dissipated per cycle)}} \tag{52}$$

For a second-order passive system, Eqs. (51) and (52) are equivalent. We will see that the Q-factor has a very simple interpretation in the magnitude Bode diagrams of second-order transfer functions.

Analytical expressions for the parameters Q and ω_0 can be found by equating like powers of s in the original transfer function, Eq. (44), and in the normalized form, Eq. (50). The result is

$$\begin{aligned} f_0 &= \frac{\omega_0}{2\pi} = \frac{1}{2\pi\sqrt{LC}} \\ Q &= R\sqrt{\frac{C}{L}} \end{aligned} \tag{53}$$

The roots s_1 and s_2 of Eqs. (47) and (48) are real when $Q \leq 0.5$, and are complex when $Q > 0.5$.

The magnitude of G is

$$\left\| G(j\omega) \right\| = \frac{1}{\sqrt{\left(1 - \left(\frac{\omega}{\omega_0}\right)^2\right)^2 + \frac{1}{Q^2}\left(\frac{\omega}{\omega_0}\right)^2}} \tag{54}$$

Asymptotes of $\|G\|$ are illustrated in Fig. 16. At low frequencies, $(\omega/\omega_0) << 1$, and hence

$$\left\| G \right\| \to 1 \quad \text{for } \omega << \omega_0 \tag{55}$$

At high frequencies, $(\omega/\omega_0) >> 1$, the $(\omega/\omega_0)^4$ term dominates the expression inside the radical of Eq. (54). Hence, the high-frequency asymptote is

$$\left\| G \right\| \to \left(\frac{f}{f_0}\right)^{-2} \quad \text{for } \omega >> \omega_0 \tag{56}$$

This expression coincides with Eq. (3), with $n = -2$. Therefore, the high-frequency asymptote has slope –40dB/decade. The asymptotes intersect at $f = f_0$, and are independent of Q.

The parameter Q affects the deviation of the actual curve from the asymptotes, in the neighborhood of the corner frequency f_0. The exact magnitude at $f = f_0$ is found by

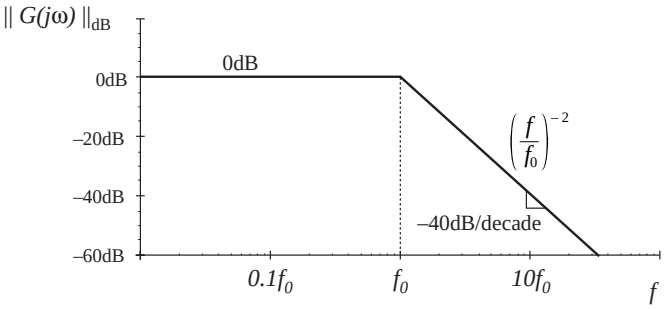

Fig. 16. Magnitude asymptotes for the two-pole transfer function.

substitution of $\omega = \omega_0$ into Eq. (8-57):

$$\left\| G(j\omega_0) \right\| = Q \tag{57}$$

So the exact transfer function has magnitude Q at the corner frequency f_0. In decibels, Eq. (57) is

$$\left\| G(j\omega_0) \right\|_{\text{dB}} = \left| Q \right|_{\text{dB}} \tag{58}$$

So if, for example, $Q = 2 \Rightarrow$ 6dB, then the actual curve deviates from the asymptotes by 6dB at the corner frequency $f = f_0$. Salient features of the magnitude Bode plot of the second-order transfer function are summarized in Fig. 17.

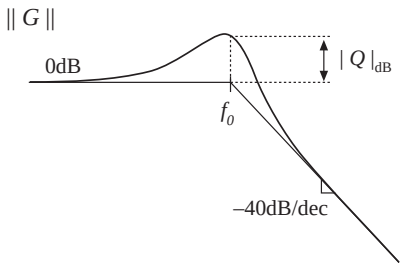

Fig. 17. Important features of the magnitude Bode plot, for the two-pole transfer function.

The phase of G is

$$\angle G(j\omega) = -\tan^{-1}\left[\frac{\frac{1}{Q}\left(\frac{\omega}{\omega_0}\right)}{1-\left(\frac{\omega}{\omega_0}\right)^2}\right] \tag{59}$$

The phase tends to 0˚ at low frequency, and to –180˚ at high frequency. At $f = f_0$, the phase is –90˚. As illustrated in Fig. 18, increasing the value of Q causes a sharper phase change between the 0˚ and –180˚ asymptotes. We again need a midfrequency asymptote, to approximate the phase transition in the vicinity of the corner frequency f_0, as illustrated in Fig. 19. As in the case of the real single pole, we could choose the slope of this asymptote to be identical to the slope of the actual curve at $f = f_0$. It can be shown that this choice leads to the following asymptote break frequencies:

$$f_a = \left(e^{\pi/2}\right)^{-\frac{1}{2Q}} f_0$$
$$f_b = \left(e^{\pi/2}\right)^{\frac{1}{2Q}} f_0 \tag{60}$$

A better choice, which is consistent with the approximation (23) used for the real single pole, is

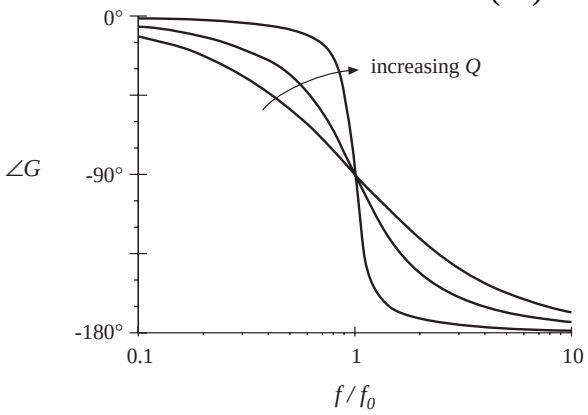

Fig. 18. Phase plot, second-order poles. Increasing Q causes a sharper phase change.

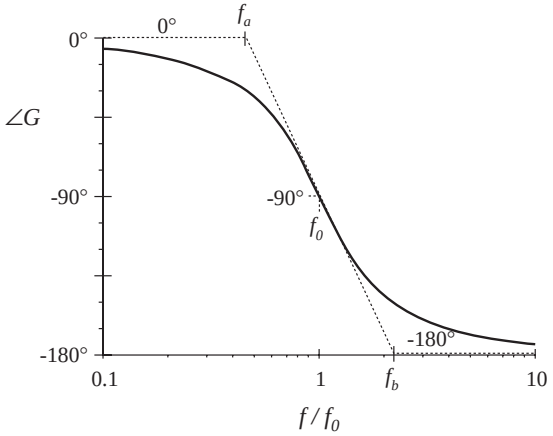

Fig. 19. One choice for the midfrequency phase asymptote of the two-pole response, which correctly predicts the actual slope at $f = f_0$.

$$f_a = 10^{-1/2Q} f_0$$
$$f_b = 10^{1/2Q} f_0 \qquad (61)$$

With this choice, the midfrequency asymptote has slope $-180Q$ degrees per decade. The phase asymptotes are summarized in Fig. 20. With $Q = 0.5$, the phase changes from 0˚ to –180˚ over a frequency span of approximately two decades, centered at the corner frequency f_0. Increasing the Q causes this frequency span to decrease rapidly.

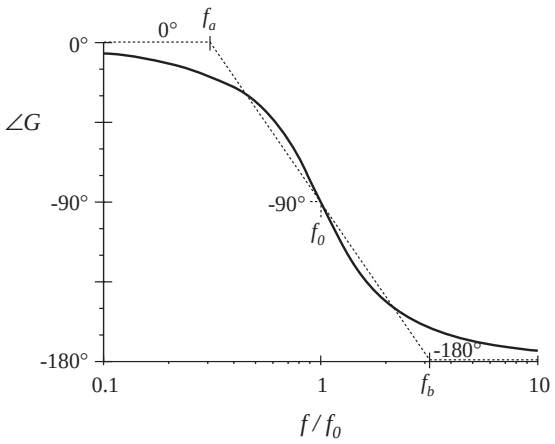

Fig. 20. A simpler choice for the midfrequency phase asymptote, which better approximates the curve over the entire frequency range and is consistent with the asymptote used for real poles.

Second-order response magnitude curves, Eq. (54), and phase curves, Eq. (59), are plotted in Figs. 21 and 22 for several values of Q.

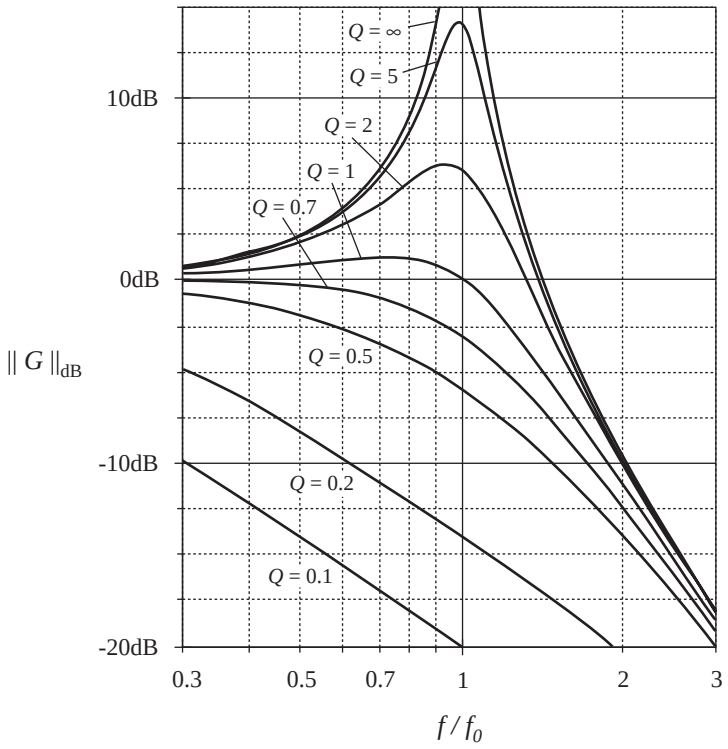

Fig. 21. Exact magnitude curves, two-pole response, for several values of Q.

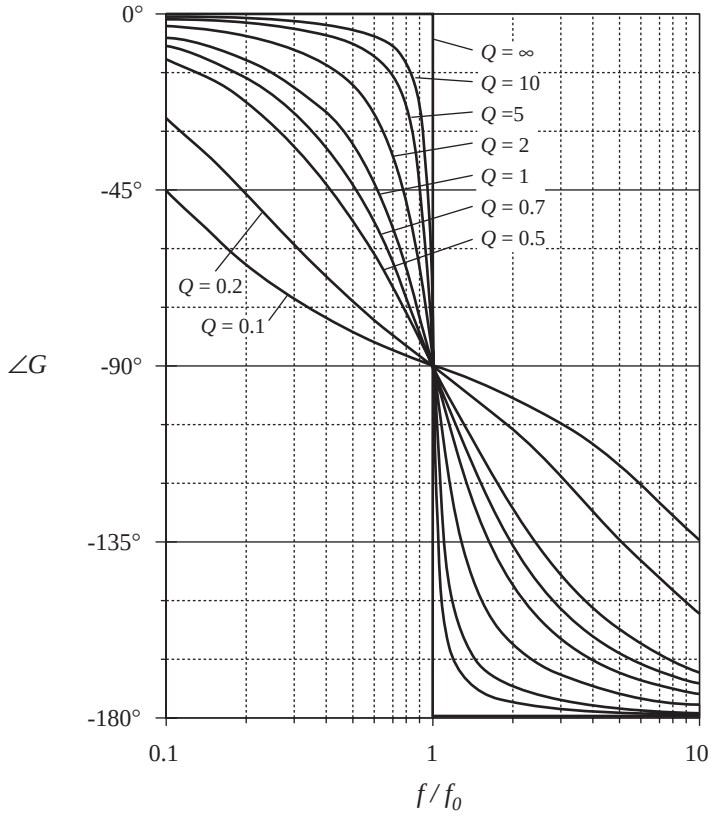

Fig. 22. Exact phase curves, two-pole response, for several values of Q.

1.6. The low-Q approximation

As mentioned in section 1.5, when the roots of second-order denominator polynomial of Eq. (45) are real, then we can factor the denominator, and construct the Bode diagram using the asymptotes for real poles. We would then use the following normalized form:

$$G(s) = \frac{1}{\left(1 + \frac{s}{\omega_1}\right)\left(1 + \frac{s}{\omega_2}\right)} \tag{61}$$

This is a particularly desirable approach when the corner frequencies ω_1 and ω_2 are well-separated in value.

The difficulty in this procedure lies in the complexity of the quadratic formula used to find the corner frequencies. Expressing the corner frequencies ω_1 and ω_2 in terms of the circuit elements R, L, C, etc., invariably leads to complicated and unilluminating expressions, especially when the circuit contains many elements. Even in the case of the simple circuit of Fig. 15, whose transfer function is given by Eq. (44), the conventional quadratic formula leads to the following complicated formula for the corner frequencies:

$$\omega_1, \omega_2 = \frac{L/R \pm \sqrt{\left(L/R\right)^2 - 4LC}}{2LC} \tag{62}$$

This equation yields essentially no insight regarding how the corner frequencies depend on the element values. For example, it can be shown that when the corner frequencies are well-separated in value, they can be expressed with high accuracy by the much simpler relations

$$\omega_1 \approx \frac{R}{L}, \qquad \omega_2 \approx \frac{1}{RC} \tag{63}$$

In this case, ω_1 is essentially independent of the value of C, and ω_2 is essentially independent of L, yet Eq. (62) apparently predicts that both corner frequencies are dependent on all element values. The simple expressions of Eq. (63) are far preferable to Eq. (62), and can be easily derived using the low-Q approximation [2].

Let us assume that the transfer function has been expressed in the standard normalized form of Eq. (50), reproduced below:

$$G(s) = \frac{1}{1 + \frac{s}{Q\omega_0} + \left(\frac{s}{\omega_0}\right)^2} \tag{64}$$

For $Q \leq 0.5$, let us use the quadratic formula to write the real roots of the denominator polynomial of Eq. (64) as

$$\omega_1 = \frac{\omega_0}{Q}\,\frac{1-\sqrt{1-4Q^2}}{2} \qquad (65)$$

$$\omega_2 = \frac{\omega_0}{Q}\,\frac{1+\sqrt{1-4Q^2}}{2} \qquad (66)$$

The corner frequency ω_2 can be expressed

$$\omega_2 = \frac{\omega_0}{Q}\,F(Q) \qquad (67)$$

where *F(Q)* is defined as

$$F(Q) = \frac{1}{2}\left(1+\sqrt{1-4Q^2}\right) \qquad (68)$$

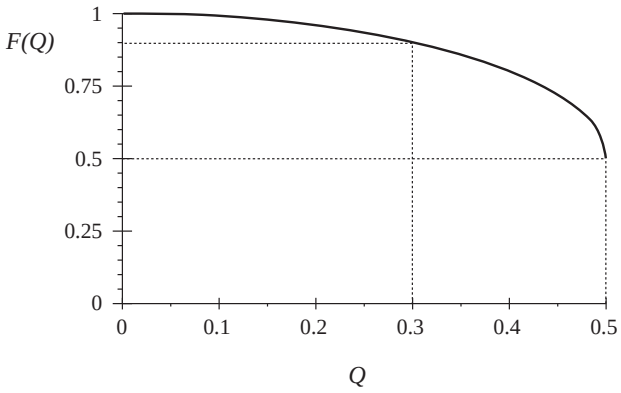

Fig. 23. *F(Q)* vs. *Q*, as given by Eq. (8-72). The approximation $F(Q) \approx 1$ is within 10% of the exact value for $Q < 0.3$.

Note that, when $Q << 0.5$, then $4Q^2 << 1$, and *F(Q)* is approximately equal to 1. We then obtain

$$\omega_2 \approx \frac{\omega_0}{Q} \quad \text{for } Q << \frac{1}{2} \qquad (69)$$

The function *F(Q)* is plotted in Fig. 23. It can be seen that *F(Q)* approaches 1 very rapidly as *Q* decreases below 0.5.

To derive a similar approximation for ω_1, we can multiply and divide Eq. (65) by *F(Q)*, Eq. (68). Upon simplification of the numerator, we obtain

$$\omega_1 = \frac{Q\,\omega_0}{F(Q)} \qquad (70)$$

Again, *F(Q)* tends to 1 for small *Q*. Hence, ω_1 can be approximated as

$$\omega_1 \approx Q\,\omega_0 \quad \text{for } Q << \frac{1}{2} \qquad (71)$$

Magnitude asymptotes for the low-*Q* case are summarized in Fig. 24. For $Q < 0.5$, the two poles at ω_0 split into real poles. One real pole occurs at corner frequency $\omega_1 < \omega_0$, while the other occurs at corner frequency $\omega_2 > \omega_0$. The corner frequencies are easily approximated, using Eqs. (69) and (71).

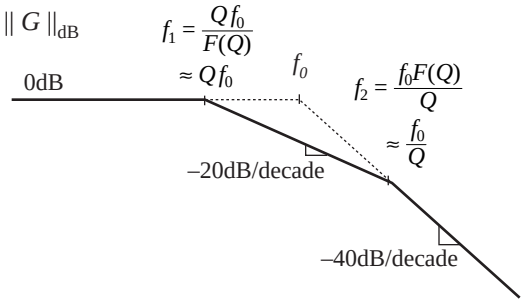

Fig. 24. Magnitude asymptotes predicted by the low-*Q* approximation. Real poles occur at frequencies Qf_0 and f_0/Q.

For the filter circuit of Fig. 15, the parameters *Q* and ω_0 are given by Eq. (53). For the case when $Q << 0.5$, we can derive the following analytical expressions for the corner frequencies, using Eqs. (70) and (71):

$$\omega_1 \approx Q\,\omega_0 = R\sqrt{\frac{C}{L}}\,\frac{1}{\sqrt{LC}} = \frac{R}{L}$$
$$\omega_2 \approx \frac{\omega_0}{Q} = \frac{1}{\sqrt{LC}}\,\frac{1}{R\sqrt{\frac{C}{L}}} = \frac{1}{RC} \qquad (72)$$

So the low-Q approximation allows us to derive simple design-oriented analytical expressions for the corner frequencies.

1.7. Approximate roots of an arbitrary-degree polynomial

The low-Q approximation can be generalized, to find approximate analytical expressions for the roots of the n^{th}-order polynomial

$$P(s) = 1 + a_1 s + a_2 s^2 + \cdots + a_n s^n \qquad (73)$$

It is desired to factor the polynomial *P(s)* into the form

$$P(s) = \left(1 + \tau_1 s\right)\left(1 + \tau_2 s\right)\cdots\left(1 + \tau_n s\right) \qquad (74)$$

In a real circuit, the coefficients $a_1,...,a_n$ are real, while the time constants $\tau_1,...,\tau_n$ may be either real or complex. Very often, some or all of the time constants are well separated in value, and depend in a very simple way on the circuit element values. In such cases, simple approximate analytical expressions for the time constants can be derived.

The time constants $\tau_1,...,\tau_n$ can be related to the original coefficients $a_1,...,a_n$ by multiplying out Eq. (74). The result is

$$\begin{aligned}
a_1 &= \tau_1 + \tau_2 + \cdots + \tau_n \\
a_2 &= \tau_1\left(\tau_2 + \cdots + \tau_n\right) + \tau_2\left(\tau_3 + \cdots + \tau_n\right) + \cdots \\
a_3 &= \tau_1\tau_2\left(\tau_3 + \cdots + \tau_n\right) + \tau_2\tau_3\left(\tau_4 + \cdots + \tau_n\right) + \cdots \\
&\vdots \\
a_n &= \tau_1\tau_2\tau_3\cdots\tau_n
\end{aligned} \qquad (75)$$

General solution of this system of equations amounts to exact factoring of the arbitrary degree polynomial, a hopeless task. Nonetheless, Eq. (75) does suggest a way to approximate the roots.

Suppose that all of the time constants $\tau_1,...,\tau_n$ are real and well separated in value. We can further assume, without loss of generality, that the time constants are arranged in decreasing order of magnitude:

$$\left|\tau_1\right| >> \left|\tau_2\right| >> \cdots >> \left|\tau_n\right| \qquad (76)$$

When the inequalities of Eq. (76) are satisfied, then the expressions for $a_1,...,a_n$ of Eq. (75) are each dominated by their first terms:

$$\begin{aligned} a_1 &\approx \tau_1 \\ a_2 &\approx \tau_1\tau_2 \\ a_3 &\approx \tau_1\tau_2\tau_3 \\ &\vdots \\ a_n &= \tau_1\tau_2\tau_3\cdots\tau_n \end{aligned} \tag{77}$$

These expressions can now be solved for the time constants, with the result

$$\begin{aligned} \tau_1 &\approx a_1 \\ \tau_2 &\approx \frac{a_2}{a_1} \\ \tau_3 &\approx \frac{a_3}{a_2} \\ &\vdots \\ \tau_n &\approx \frac{a_n}{a_{n-1}} \end{aligned} \tag{78}$$

Hence, if

$$\left|a_1\right| >> \left|\frac{a_2}{a_1}\right| >> \left|\frac{a_3}{a_2}\right| >> \cdots >> \left|\frac{a_n}{a_{n-1}}\right| \tag{79}$$

then the polynomial *P(s)* given by Eq. (73) has the approximate factorization

$$P(s) \approx \left(1 + a_1 s\right)\left(1 + \frac{a_2}{a_1} s\right)\left(1 + \frac{a_3}{a_2} s\right)\cdots\left(1 + \frac{a_n}{a_{n-1}} s\right) \tag{80}$$

Note that if the original coefficients in Eq. (73) are simple functions of the circuit elements, then the approximate roots given by Eq. (80) are similar simple functions of the circuit elements. So approximate analytical expressions for the roots can be obtained. Numerical values are substituted into Eq. (79) to justify the approximation.

In the case where two of the roots are not well separated, then one of the inequalities of Eq. (79) is violated. We can then leave the corresponding terms in quadratic form. For example, suppose that inequality *k* is not satisfied:

$$\left|a_1\right| >> \left|\frac{a_2}{a_1}\right| >> \cdots >> \left|\frac{a_k}{a_{k-1}}\right| \quad \not>> \quad \left|\frac{a_{k+1}}{a_k}\right| >> \cdots >> \left|\frac{a_n}{a_{n-1}}\right| \tag{81}$$

↑
not
satisfied

Then an approximate factorization is

$$P(s) \approx \left(1 + a_1 s\right)\left(1 + \frac{a_2}{a_1} s\right) \cdots \left(1 + \frac{a_k}{a_{k-1}} s + \frac{a_{k+1}}{a_{k-1}} s^2\right) \cdots \left(1 + \frac{a_n}{a_{n-1}} s\right) \tag{82}$$

The conditions for accuracy of this approximation are

$$\left|a_1\right| >> \left|\frac{a_2}{a_1}\right| >> \cdots >> \left|\frac{a_k}{a_{k-1}}\right| >> \left|\frac{a_{k-2}\, a_{k+1}}{a_{k-1}^2}\right| >> \cdots >> \left|\frac{a_n}{a_{n-1}}\right| \tag{83}$$

Complex conjugate roots can be approximated in this manner.

When the first inequality of Eq. (79) is violated, i.e.,

$$\left|a_1\right| \not>> \left|\frac{a_2}{a_1}\right| >> \left|\frac{a_3}{a_2}\right| >> \cdots >> \left|\frac{a_n}{a_{n-1}}\right|$$

↑ not satisfied

(84)

then the first two roots should be left in quadratic form:

$$P(s) \approx \left(1 + a_1 s + a_2 s^2\right)\left(1 + \frac{a_3}{a_2} s\right) \cdots \left(1 + \frac{a_n}{a_{n-1}} s\right) \tag{85}$$

This approximation is justified provided that

$$\left|\frac{a_2^2}{a_3}\right| >> \left|a_1\right| >> \left|\frac{a_3}{a_2}\right| >> \left|\frac{a_4}{a_3}\right| >> \cdots >> \left|\frac{a_n}{a_{n-1}}\right| \tag{86}$$

If none of the above approximations is justified, then there are three or more roots that are close in magnitude. One must then resort to cubic or higher-order forms.

As an example, consider the following transfer function:

$$G(s) = \frac{G_0}{1 + s\,\frac{L_1 + L_2}{R} + s^2 L_1 C + s^3\,\frac{L_1 L_2 C}{R}} \tag{87}$$

This transfer function contains a third-order denominator, with the following coefficients:

$$a_1 = \frac{L_1 + L_2}{R}$$

$$a_2 = L_1 C$$

$$a_3 = \frac{L_1 L_2 C}{R} \tag{88}$$

It is desired to factor the denominator, to obtain analytical expressions for the poles. The correct way to do this depends on the numerical values of R, L_1, L_2, and C. When the roots are real and well separated, then Eq. (80) predicts that the denominator can be factored as follows:

$$\left(1 + s\,\frac{L_1 + L_2}{R}\right)\left(1 + sRC\,\frac{L_1}{L_1 + L_2}\right)\left(1 + s\,\frac{L_2}{R}\right) \tag{89}$$

According to Eq. (79), this approximation is justified provided that

$$\frac{L_1 + L_2}{R} >> RC\,\frac{L_1}{L_1 + L_2} >> \frac{L_2}{R} \tag{90}$$

These inequalities cannot be satisfied unless $L_1 >> L_2$. When $L_1 >> L_2$, then Eq. (90) can be further simplified to

$$\frac{L_1}{R} >> RC >> \frac{L_2}{R} \tag{91}$$

The approximate factorization, Eq. (89), can then be further simplified to

$$\left(1 + s\,\frac{L_1}{R}\right)\left(1 + sRC\right)\left(1 + s\,\frac{L_2}{R}\right) \tag{92}$$

Thus, in this case the transfer function contains three well separated real poles.

When the second inequality of Eq. (90) is violated,

$$\frac{L_1 + L_2}{R} >> RC\,\frac{L_1}{L_1 + L_2} \quad \not> \quad \frac{L_2}{R}$$

$$\uparrow$$

not satisfied

(93)

then the second and third roots should be left in quadratic form:

$$\left(1 + s\,\frac{L_1 + L_2}{R}\right)\left(1 + sRC\,\frac{L_1}{L_1 + L_2} + s^2\,L_1 \| L_2\,C\right) \tag{94}$$

This expression follows from Eq. (82), with $k = 2$. Equation (83) predicts that this approximation is justified provided that

$$\frac{L_1 + L_2}{R} >> RC\,\frac{L_1}{L_1 + L_2} >> \frac{L_1 \| L_2}{L_1 + L_2}\,RC \tag{95}$$

In application of Eq. (83), we take a_0 to be equal to 1. The inequalities of Eq. (95) can be simplified to obtain

$$L_1 >> L_2, \quad \text{and} \quad \frac{L_1}{R} >> RC \tag{96}$$

Note that it is no longer required that $RC >> L_2 / R$. Equation (96) implies that factorization (94) can be further simplified to

$$\left(1 + s\,\frac{L_1}{R}\right)\left(1 + sRC + s^2 L_2 C\right) \tag{97}$$

Thus, for this case, the transfer function contains a low-frequency pole that is well separated from a high-frequency quadratic pole pair.

In the case where the first inequality of Eq. (90) is violated:

$$\frac{L_1 + L_2}{R} \not>> RC\frac{L_1}{L_1 + L_2} >> \frac{L_2}{R} \qquad \uparrow \text{ not satisfied} \tag{98}$$

then the first and second roots should be left in quadratic form:

$$\left(1 + s\frac{L_1 + L_2}{R} + s^2 L_1 C\right)\left(1 + s\frac{L_2}{R}\right) \tag{99}$$

This expression follows directly from Eq. (85). Equation (86) predicts that this approximation is justified provided that

$$\frac{L_1 RC}{L_2} >> \frac{L_1 + L_2}{R} >> \frac{L_2}{R} \tag{100}$$

i.e.,

$$L_1 >> L_2, \quad \text{and} \quad RC >> \frac{L_2}{R} \tag{101}$$

For this case, the transfer function contains a low-frequency quadratic pole pair that is well-separated from a high-frequency real pole. If none of the above approximations are justified, then all three of the roots are similar in magnitude. We must then find other means of dealing with the original cubic polynomial.

2. Analysis of transfer functions —example

Let us next derive analytical expressions for the poles, zeroes, and asymptote gains in the transfer functions of a given example.

The differential equations of the a certain given system are:

$$\begin{aligned} L\frac{di(t)}{dt} &= -Dv_g(t) + (1-D)v(t) + \left(V_g - V\right)v_c(t) \\ C\frac{dv(t)}{dt} &= -(1-D)\,i(t) - \frac{v(t)}{R} + Iv_c(t) \\ i_g(t) &= Di(t) + Iv_c(t) \end{aligned} \tag{102}$$

The system contains two independent ac inputs: the control input $v_c(t)$ and the input voltage $v_g(t)$. The capitalized quantities are given constants. In the Laplace transform domain, the ac output voltage $v(s)$ can be expressed as the superposition of terms arising from the two inputs:

$$v(s) = G_{vc}(s)\,v_c(s) + G_{vg}(s)\,v_g(s) \tag{103}$$

Hence, the transfer functions $G_{vc}(s)$ and $G_{vg}(s)$ can be defined as

$$G_{vc}(s) = \left.\frac{v(s)}{v_c(s)}\right|_{v_g(s)=0} \quad \text{and} \quad G_{vg}(s) = \left.\frac{v(s)}{v_g(s)}\right|_{v_c(s)=0} \tag{104}$$

An algebraic approach to deriving these transfer functions begins by taking the Laplace transform of Eq. (102), letting the initial conditions be zero:

$$\begin{aligned} sL\, i(s) &= -D\, v_g(s) + (1-D)\, v(s) + \left(V_g - V\right) v_c(s) \\ sC\, v(s) &= -(1-D)\, i(s) - \frac{v(s)}{R} + I\, v_c(s) \end{aligned} \tag{105}$$

To solve for the output voltage $v(s)$, we can use the top equation to eliminate $i(s)$:

$$i(s) = \frac{-D\, v_g(s) + (1-D)\, v(s) + \left(V_g - V\right) v_c(s)}{sL} \tag{106}$$

Substitution of this expression into the lower equation of (105) leads to

$$sCv(s) = -\frac{(1-D)}{sL}\left(-D\, v_g(s) + (1-D)\, v(s) + \left(V_g - V\right) v_c(s)\right) - \frac{v(s)}{R} + I\, v_c(s) \tag{107}$$

Solution for $v(s)$ results in

$$v(s) = \frac{D(1-D)}{(1-D)^2 + s\frac{L}{R} + s^2 LC}\, v_g(s) - \frac{V_g - V - s\,LI}{(1-D)^2 + s\frac{L}{R} + s^2 LC}\, v_c(s) \tag{108}$$

We aren't done yet —the next step is to manipulate these expressions into normalized form, such that the coefficients of s^0 in the numerator and denominator polynomials are equal to one:

$$\begin{aligned} v(s) = &\left(\frac{D}{1-D}\right) \frac{1}{1 + s\frac{L}{(1-D)^2 R} + s^2 \frac{LC}{(1-D)^2}}\, v_g(s) \\ &- \left(\frac{V_g - V}{(1-D)^2}\right) \frac{\left(1 - s\frac{LI}{V_g - V}\right)}{1 + s\frac{L}{(1-D)^2 R} + s^2 \frac{LC}{(1-D)^2}}\, v_c(s) \end{aligned} \tag{109}$$

This result is similar in form to Eq. (103). The transfer function from $v_g(s)$ to $v(s)$ is

$$G_{vg}(s) = \left.\frac{v(s)}{v_g(s)}\right|_{v_c(s)=0} = \left(\frac{D}{1-D}\right) \frac{1}{1 + s\frac{L}{(1-D)^2 R} + s^2 \frac{LC}{(1-D)^2}} \tag{110}$$

Thus, this transfer function contains a dc gain G_{g0} and a quadratic pole pair:

$$G_{vg}(s) = G_{g0} \frac{1}{1 + \frac{s}{Q\omega_0} + \left(\frac{s}{\omega_0}\right)^2} \tag{111}$$

Analytical expressions for the salient features of the transfer function from $v_g(s)$ to $v(s)$ are found by equating like terms in Eqs. (110) and (111). The dc gain is

$$G_{g0} = \frac{D}{1 - D} \tag{112}$$

By equating the coefficients of s^2 in the denominators of Eqs. (110) and (111), one obtains

$$\frac{1}{\omega_0^2} = \frac{LC}{D'^2} \tag{113}$$

Hence, the angular corner frequency is

$$\omega_0 = \frac{D'}{\sqrt{LC}} \tag{114}$$

By equating coefficients of s in the denominators of Eqs. (110) and (111), one obtains

$$\frac{1}{Q\omega_0} = \frac{L}{D'^2 R} \tag{115}$$

Elimination of ω_0 using Eq. (114) and solution for Q leads to

$$Q = D'R\sqrt{\frac{C}{L}} \tag{116}$$

Equations (114), (112), and (116) are the desired results in the analysis of the voltage transfer function from $v_g(s)$ to $v(s)$. These expressions are useful not only in analysis situations, where it is desired to find numerical values of the salient features G_{g0}, ω_0, and Q, but also in design situations, where it is desired to select numerical values for R, L, and C such that given values of the salient features are obtained.

Having found analytical expressions for the salient features of the transfer function, we can now plug in numerical values and construct the Bode plot. Suppose that we are given the following values:

$$\begin{aligned} D &= 0.6 \\ R &= 10\Omega \\ V_g &= 30\text{V} \\ L &= 160\mu\text{H} \\ C &= 160\mu\text{F} \end{aligned} \tag{117}$$

We can evaluate Eqs. (112), (114), and (116), to determine numerical values of the salient features of the transfer functions. The results are:

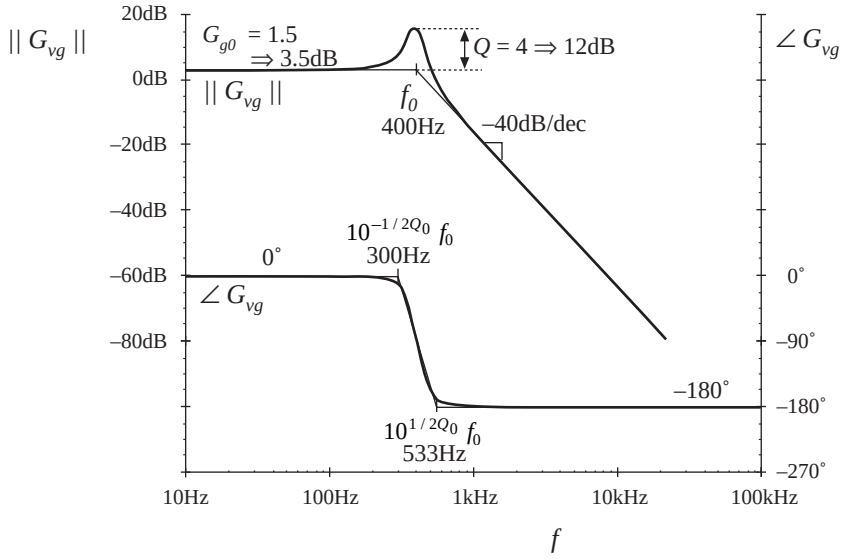

Fig. 25. Bode plot of the transfer function G_{va}.

$$\left|G_{g0}\right| = \frac{D}{1-D} = 1.5 \Rightarrow 3.5\text{dB}$$
$$f_0 = \frac{\omega_0}{2\pi} = \frac{D'}{2\pi\sqrt{LC}} = 400\text{Hz}$$
$$Q = D'R\sqrt{\frac{C}{L}} = 4 \Rightarrow 12\text{dB} \qquad (118)$$

The Bode plot of the magnitude and phase of the transfer function G_{vg} is constructed in Fig. 25. This transfer function contains a dc gain of 3.5dB and resonant poles at 400Hz having a Q of 4 ⇒ 12dB. The resonant poles contribute –180˚ to the high frequency phase asymptote.

3. Graphical construction of transfer functions

Often, we can draw approximate Bode diagrams by inspection, without large amounts of messy algebra and the inevitable associated algebra mistakes. A great deal of insight can be gained into the operation of the circuit using this method. It becomes clear which components dominate the circuit response at various frequencies, and so suitable approximations become obvious. Analytical expressions for the approximate corner frequencies and asymptotes can be obtained directly. Impedances and transfer functions of quite complicated networks can be constructed. Thus insight can be gained, so that the design engineer can modify the circuit to obtain a desired frequency response.

The graphical construction method, also known as “doing algebra on the graph”, involves use of a few simple rules for combining the magnitude Bode plots of impedances and transfer functions.

3.1. Series impedances: addition of asymptotes

A series connection represents the addition of impedances. If the Bode diagrams of the individual impedance magnitudes are known, then the asymptotes of the series combination are found by simply taking the largest of the individual impedance asymptotes. In many cases, the result is exact. In other cases, such as when the individual asymptotes have the same slope, then the result is an approximation; nonetheless, the accuracy of the approximation can be quite good.

Consider the series-connected *R*-*C* network of Fig. 26. It is desired to construct the magnitude asymptotes of the total series impedance *Z(s)*, where

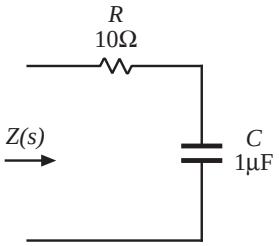

Fig. 26. Series *R*-*C* network example.

$$Z(s) = R + \frac{1}{sC} \tag{119}$$

Let us first sketch the magnitudes of the individual impedances. The 10Ω resistor has an impedance magnitude of 10Ω ⇒ 20dBΩ. This value is independent of frequency, and is given in Fig. 27. The capacitor has an impedance magnitude of 1/ω*C*. This quantity varies inversely with ω, and hence its magnitude Bode plot is a line with slope –20dB/decade. The line passes through 1Ω ⇒ 0dBΩ at the angular frequency ω where

$$\frac{1}{\omega C} = 1\Omega \tag{120}$$

i.e., at

$$\omega = \frac{1}{1\Omega\, C} = \frac{1}{(1\Omega)\,(10^{-6}\text{F})} = 10^6 \text{ rad/sec} \tag{121}$$

In terms of frequency *f*, this occurs at

$$f = \frac{\omega}{2\pi} = \frac{10^6}{2\pi} = 159\text{kHz} \tag{122}$$

So the capacitor impedance magnitude is a line with slope –20dB/dec, and which passes through 0dBΩ at 159kHz, as shown in Fig. 27. It should be noted that, for simplicity, the asymptotes in Fig. 27 have been labeled *R* and 1/ω*C*. But to draw the Bode plot, we must actually plot dBΩ; e.g., 20 $\log_{10}$ (*R*/1Ω) and 20 $\log_{10}$ ((1/ω*C*)/1Ω).

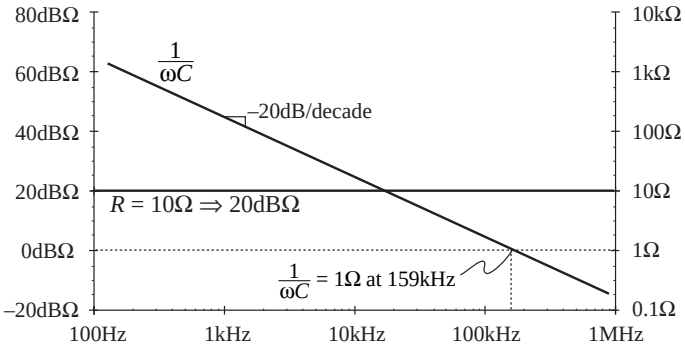

Fig. 27. Impedance magnitudes of the individual elements in the network of Fig. 26.

Let us now construct the magnitude of *Z(s)*, given by Eq. (119). The magnitude of *Z* can be approximated as follows:

$$\left\| Z(j\omega) \right\| = \left\| R + \frac{1}{j\omega C} \right\| \approx \begin{cases} R & \text{for } R >> 1 / \omega C \\ \dfrac{1}{\omega C} & \text{for } R << 1 / \omega C \end{cases} \tag{123}$$

The asymptotes of the series combination are simply the larger of the individual resistor and capacitor asymptotes, as illustrated by the heavy lines in Fig 28. For this example, these are in fact the exact asymptotes of $\| Z \|$. In the limiting case of zero frequency (dc), then the capacitor tends to an open circuit. The series combination is then dominated by the capacitor, and the exact function tends asymptotically to the capacitor impedance magnitude. In the limiting case of infinite frequency, then the capacitor tends to a short circuit, and the total impedance becomes simply *R*. So the *R* and $1/\omega C$ lines are the exact asymptotes for this example.

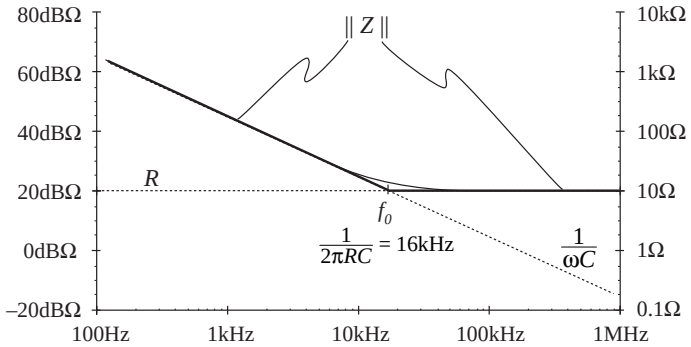

Fig. 28. Construction of the composite asymptotes of $\| Z \|$. The asymptotes of the series combination can be approximated by simply selecting the larger of the individual resistor and capacitor asymptotes.

The corner frequency f_0, where the asymptotes intersect, can now be easily deduced. At angular frequency $\omega_0 = 2\pi f_0$, the two asymptotes are equal in value:

$$\frac{1}{\omega_0 C} = R \tag{124}$$

Solution for ω_0 and f_0 leads to:

$$\omega_0 = \frac{1}{RC} = \frac{1}{(10\Omega)\,(10^{-6}\text{F})} = 10^5 \text{ rad/sec} \tag{125}$$

$$f_0 = \frac{\omega_0}{2\pi} = \frac{1}{2\pi RC} = 16\text{kHz}$$

So if we can write analytical expressions for the asymptotes, then we can equate the expressions to find analytical expressions for the corner frequencies where the asymptotes intersect.

The deviation of the exact curve from the asymptotes follows all of the usual rules. The slope of the asymptotes changes by +20dB/decade at the corner frequency f_0 (i.e., from –20dBΩ/decade to 0dBΩ/decade), and hence there is a zero at $f = f_0$. So the exact

curve deviates from the asymptotes by +3dBΩ at $f = f_0$, and by +1dBΩ at $f = 2f_0$ and at $f = f_0/2$.

As a second example, let us construct the magnitude asymptotes for the series *R-L-C* circuit of Fig. 29. The series impedance *Z(s)* is

$$Z(s) = R + sL + \frac{1}{sC} \tag{126}$$

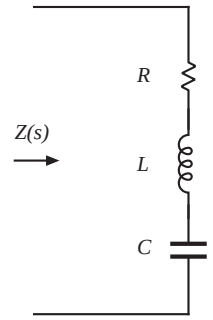

Fig. 29. Series *R-L-C* network example.

The magnitudes of the individual resistor, inductor, and capacitor asymptotes are plotted in Fig. 30, for the values

$$R = 1\text{k}\Omega$$
$$L = 1\text{mH}$$
$$C = 0.1\mu\text{F} \tag{127}$$

The series impedance *Z(s)* is dominated by the capacitor at low frequency, by the resistor at mid frequencies, and by the inductor at high frequencies, as illustrated by the bold line in Fig. 30. The impedance *Z(s)* contains a zero at angular frequency ω_1, where the capacitor and resistor asymptotes intersect. By equating the expressions for the resistor and capacitor asymptotes, we can find ω_1:

$$R = \frac{1}{\omega_1 C} \quad \Rightarrow \quad \omega_1 = \frac{1}{RC} \tag{128}$$

A second zero occurs at angular frequency ω_2, where the inductor and resistor asymptotes intersect. Upon equating the expressions for the resistor and inductor asymptotes at ω_2, we obtain the following:

$$R = \omega_2 L \quad \Rightarrow \quad \omega_2 = \frac{R}{L} \tag{129}$$

So simple expressions for all important features of the magnitude Bode plot of *Z(s)* can be obtained directly. It should be noted that Eqs. (128) and (129) are approximate, rather than exact, expressions for the corner frequencies ω_1 and ω_2. Equations (128) and (129) coincide with the results obtained via the low-*Q* approximation of section 1.6.

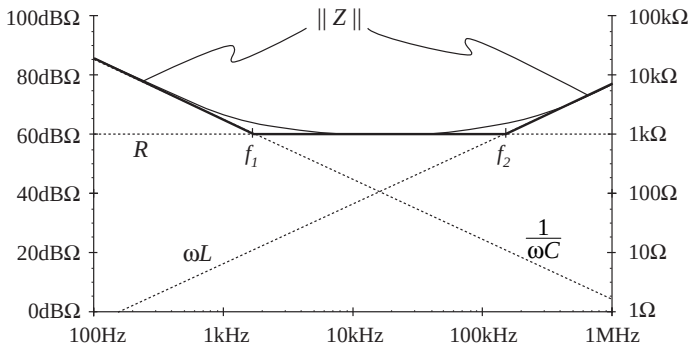

Fig. 30. Graphical construction of || *Z* || of the series *R-L-C* network of Fig. 29, for the element values specified by Eq. (127).

Next, suppose that the value of *R* is decreased to 10Ω. As *R* is reduced in value, the approximate corner frequencies ω_1 and ω_2 move closer together until, at $R = 100\Omega$, they

are both 100krad/sec. Reducing R further in value causes the asymptotes to become independent of the value of R, as illustrated in Fig. 31 for R = 10Ω. The $\| Z \|$ asymptotes now switch directly from ωL to $1/\omega C$.

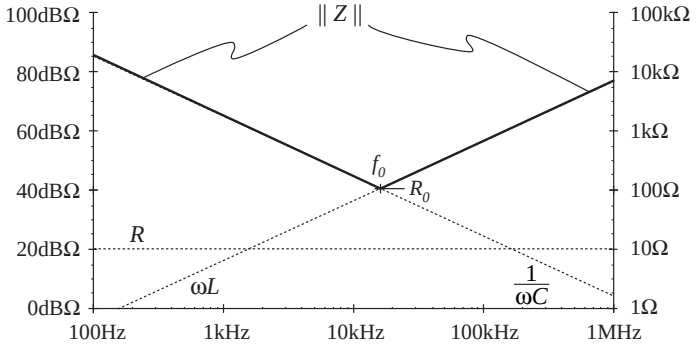

Fig. 31. Graphical construction of impedance asymptotes for the series *R-L-C* network example, with R decreased to 10Ω.

So now there are two zeroes at $\omega = \omega_0$. At corner frequency ω_0, the inductor and capacitor asymptotes are equal in value. Hence,

$$\omega_0 L = \frac{1}{\omega_0 C} = R_0 \tag{130}$$

Solution for the angular corner frequency ω_0 leads to

$$\omega_0 = \frac{1}{\sqrt{LC}} \tag{131}$$

At $\omega = \omega_0$, the inductor and capacitor impedances both have magnitude R_0, called the *characteristic impedance.*

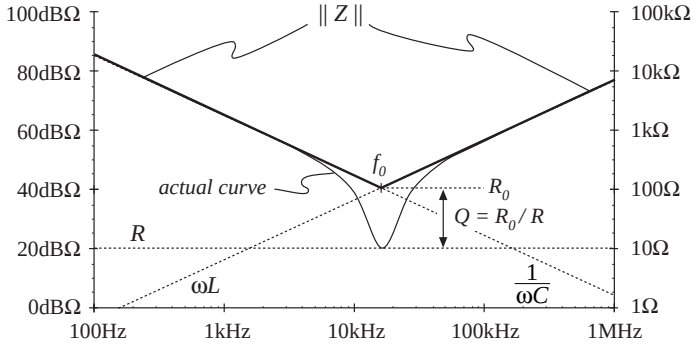

Fig. 32. Actual impedance magnitude (solid line) for the series *R-L-C* example. The inductor and capacitor impedances cancel out at $f = f_0$, and hence $Z(j\omega_0) = R$.

Since there are two zeroes at $\omega = \omega_0$, there is a possibility that the two poles could be complex conjugates, and that peaking could occur in the vicinity of $\omega = \omega_0$. So let us investigate what the actual curve does at $\omega = \omega_0$. The actual value of the series impedance $Z(j\omega_0)$ is

$$Z(j\omega_0) = R + j\omega_0 L + \frac{1}{j\omega_0 C} \tag{132}$$

Substitution of Eq. (130) into Eq. (132) leads to

$$Z(j\omega_0) = R + jR_0 + \frac{R_0}{j} = R + jR_0 - jR_0 = R \tag{133}$$

At $\omega = \omega_0$, the inductor and capacitor impedances are equal in magnitude but opposite in phase. Hence, they exactly cancel out in the series impedance, and we are left with $Z(j\omega_0) =$

R, as illustrated in Fig. 32. The actual curve in the vicinity of the resonance at $\omega = \omega_0$ can deviate significantly from the asymptotes, because its value is determined by *R* rather than ωL or $1/\omega C$.

We know from section 1.5 that the deviation of the actual curve from the asymptotes at $\omega = \omega_0$ is equal to *Q*. From Fig. 32, one can see that

$$\left| Q \right|_{\text{dB}} = \left| R_0 \right|_{\text{dB}\Omega} - \left| R \right|_{\text{dB}\Omega}, \text{ or}$$
$$Q = \frac{R_0}{R} \tag{134}$$

Equations (130) - (134) are exact results for the series resonant circuit.

The practice of adding asymptotes by simply selecting the larger asymptote can be applied to transfer functions as well as impedances. For example, suppose that we have already constructed the magnitude asymptotes of two transfer functions, G_1 and G_2, and we wish to find the asymptotes of $G = G_1 + G_2$. At each frequency, the asymptote for *G* can be approximated by simply selecting the larger of the asymptotes for G_1 and G_2:

$$G \approx \begin{cases} G_1, & \left\| G_1 \right\| >> \left\| G_2 \right\| \\ G_2, & \left\| G_2 \right\| >> \left\| G_1 \right\| \end{cases} \tag{135}$$

Corner frequencies can be found by equating expressions for asymptotes as illustrated in the preceeding examples. In the next chapter, we will see that this approach yields a simple and powerful method for determining the closed-loop transfer functions of feedback systems. The accuracy of the result is discussed in section 3.3.

3.2. Parallel impedances: inverse addition of asymptotes

A parallel combination represents inverse addition of impedances:

$$Z_{par} = \frac{1}{\frac{1}{Z_1} + \frac{1}{Z_2} + \ldots} \tag{136}$$

If the asymptotes of the individual impedances Z_1, Z_2, …, are known, then the asymptotes of the parallel combination Z_{par} can be found by simply selecting the smallest individual impedance asymptote. This is true because the smallest impedance will have the largest inverse, and will dominate the inverse sum. As in the case of the series impedances, this procedure will often yield the exact asymptotes of Z_{par}.

Let us construct the magnitude asymptotes for the parallel *R-L-C* network of Fig. 33, using the following element values:

$R = 10\Omega$

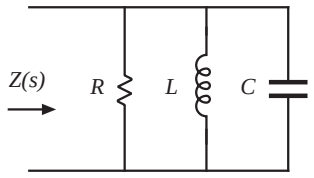

Fig. 33. Parallel *R-L-C* network example.

L = 1mH

C = 0.1μF (137)

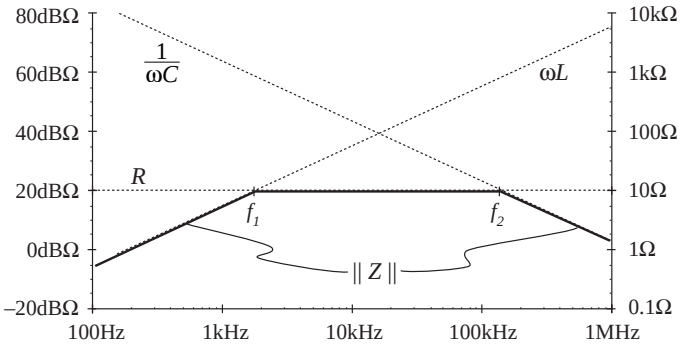

Fig. 34. Construction of the composite asymptotes of || Z ||, for the parallel R-L-C example. The asymptotes of the parallel combination can be approximated by simply selecting the smallest of the individual resistor, inductor, and capacitor asymptotes.

Impedance magnitudes of the individual elements are illustrated in Fig. 34. The asymptotes for the total parallel impedance Z are approximated by simply selecting the smallest individual element impedance, as shown by the heavy line in Fig. 34. So the parallel impedance is dominated by the inductor at low frequency, by the resistor at mid frequencies, and by the capacitor at high frequency. Approximate expressions for the angular corner frequencies are again found by equating asymptotes:

$$\begin{aligned} &\text{at } \omega = \omega_1, \quad R = \omega_1 L \quad \Rightarrow \quad \omega_1 = \frac{R}{L} \\ &\text{at } \omega = \omega_2, \quad R = \frac{1}{\omega_2 C} \quad \Rightarrow \quad \omega_2 = \frac{1}{RC} \end{aligned} \tag{138}$$

These expressions could have been obtained by conventional analysis, combined with the low-Q approximation of section 1.6.

Figure 35 illustrates what happens when the value of R is increased to 1kΩ. The asymptotes for || Z || then become independent of R, and change directly from ωL to $1/\omega C$ at angular frequency ω_0. The corner frequency ω_0 is now the frequency where the inductor and capacitor asymptotes have equal value:

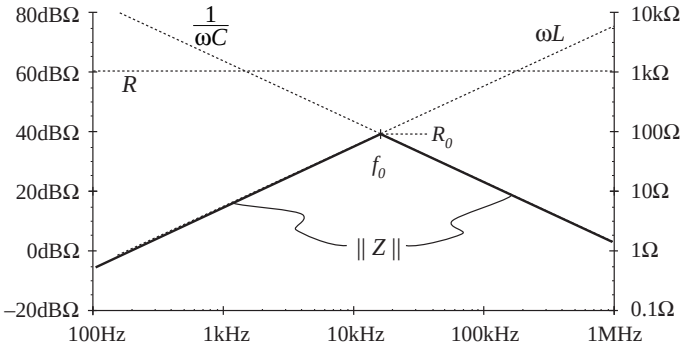

Fig. 35. Graphical construction of impedance asymptotes for the parallel R-L-C example, with R increased to 1kΩ.

$$\omega_0 L = \frac{1}{\omega_0 C} = R_0 \tag{139}$$

which implies that

$$\omega_0 = \frac{1}{\sqrt{LC}} \tag{140}$$

At ω = ω_0, the slope of the asymptotes of || *Z* || changes from +20dB/decade to –20dB/decade, and hence there are two poles. We should investigate whether peaking occurs, by determining the exact value of || *Z* || at ω = ω_0, as follows:

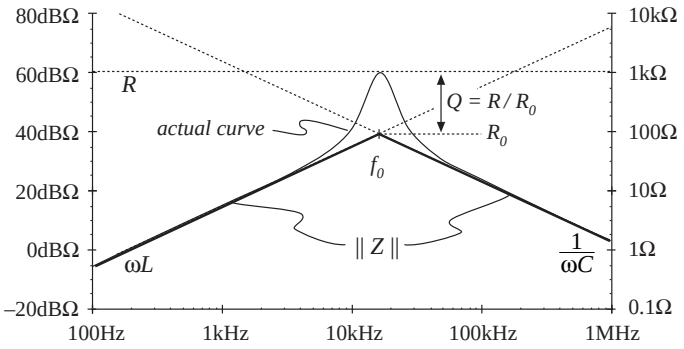

Fig. 36. Actual impedance magnitude (solid line) for the parallel *R-L-C* example. The inductor and capacitor impedances cancel out at $f = f_0$, and hence $Z(j\omega_0) = R$.

$$Z(j\omega_0) = R \parallel j\omega_0 L \parallel \frac{1}{j\omega_0 C} = \frac{1}{\frac{1}{R} + \frac{1}{j\omega_0 L} + j\omega_0 C} \tag{141}$$

Substitution of Eq. (139) into (141) yields

$$Z(j\omega_0) = \frac{1}{\frac{1}{R} + \frac{1}{jR_0} + \frac{j}{R_0}} = \frac{1}{\frac{1}{R} - \frac{j}{R_0} + \frac{j}{R_0}} = R \tag{142}$$

So at ω = ω_0, the impedances of the inductor and capacitor again cancel out, and we are left with $Z(j\omega_0) = R$. The values of *L* and *C* determine the values of the asymptotes, but *R* determines the value of the actual curve at ω = ω_0.

The actual curve is illustrated in Fig. 36. The deviation of the actual curve from the asymptotes at ω = ω_0 is

$$\left| Q \right|_{\text{dB}} = \left| R \right|_{\text{dB}\Omega} - \left| R_0 \right|_{\text{dB}\Omega}, \text{ or}$$
$$Q = \frac{R}{R_0} \tag{143}$$

Equations (139) - (143) are exact results for the parallel resonant circuit.

3.3. Another example

Now let us consider a slightly more complicated example, Fig. 37. This example illustrates the multiple application of the series and parallel rules, and it also illustrates why the algebra-on-the-graph approach in general yields approximate, rather than exact, asymptotes.

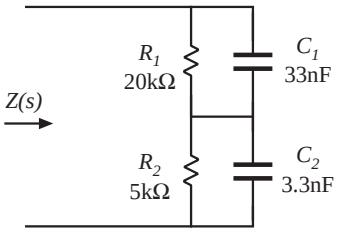

Fig. 37. Series-parallel network example.

For this circuit, the impedance *Z* consists of the series-parallel combination,

$$Z(s) = \left(R_1 \parallel \frac{1}{sC_1}\right) + \left(R_2 \parallel \frac{1}{sC_2}\right) \tag{144}$$

As usual, we first sketch the plots of the impedances of the individual elements. The result is given in Fig. 38. Next, we construct the asymptotes of the parallel combinations

$$R_1 \parallel \frac{1}{sC_1} \quad \text{and} \quad R_2 \parallel \frac{1}{sC_2}$$

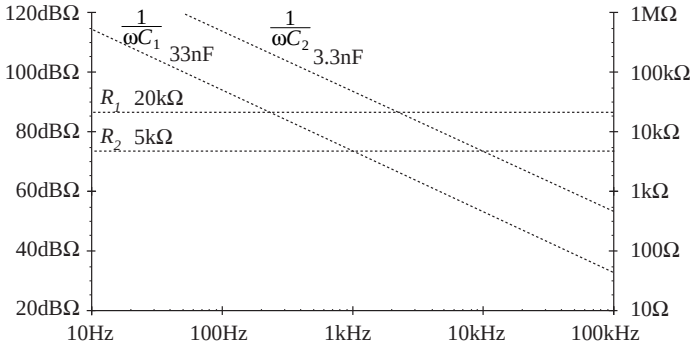

Fig. 38. Impedance magnitudes of the individual elements in the network of Fig. 37.

As before, the parallel combinations are constructed by selecting the smaller of the individual asymptotes. The result is illustrated in Fig. 39. The parallel combination of R_1 and C_1 contains a pole at frequency f_1, where the R_1 and $1/\omega C_1$ asymptotes intersect. By equating these two asymptotes at frequency f_1, we obtain

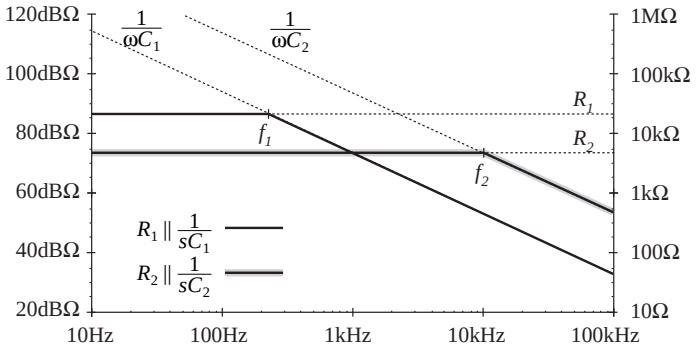

Fig. 39. Graphical construction of asymptotes for parallel combinations (solid and shaded lines).

$$R_1 = \frac{1}{\omega_1 C_1} \qquad (145)$$

Solve for $f_1 = \omega_1/2\pi$:

$$f_1 = \frac{1}{2\pi R_1 C_1} = 240\text{Hz} \qquad (146)$$

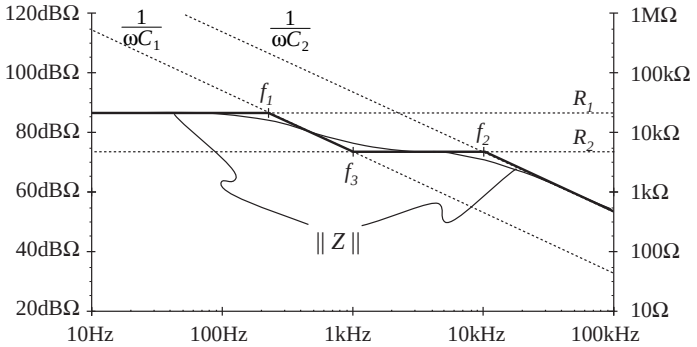

Fig. 40. Graphical construction of composite asymptotes for ∥ Z ∥.

Likewise, the parallel combination of R_2 and C_2 contains a pole at frequency f_2, where the R_2 and $1/\omega C_2$ asymptotes intersect. By equating these two asymptotes at frequency f_2 and proceeding in a similar manner, we obtain

$$f_2 = \frac{1}{2\pi R_2 C_2} = 9.6\text{kHz} \qquad (147)$$

Finally, the impedance magnitude ∥ Z ∥ is constructed as the series combination given by Eq. (144). This is done by selecting the larger of the two sets of asymptotes of Fig. 39, as illustrated in Fig. 40. Note that there is a third corner frequency: a zero occurs at frequency f_3, where the R_2 and $1/\omega C_1$ asymptotes intersect. Hence, at this corner frequency we have

$$R_2 = \frac{1}{\omega_3 C_1} \tag{148}$$

or,

$$f_3 = \frac{1}{2\pi R_2 C_1} = 965\text{Hz} \tag{149}$$

The actual curve deviates from the asymptotes, according to the usual rules. For example, at f_2, the actual curve deviates from the asymptotes by – 3dB.

The asymptotes derived in this example are approximate rather than exact. For example, the actual dc asymptote is $R_1 + R_2 = 25\text{k}\Omega$, rather than simply $R_1 = 20\text{k}\Omega$. This can be seen from the original circuit, letting the two capacitors become open circuits. On a dB scale, 25kΩ represents 28dBkΩ while 20kΩ represents 26dBkΩ, so the approximate dc asymptote deviates by 2dB from the exact value. Likewise, the high-frequency asymptote should be

$$\frac{1}{\omega\left(\frac{C_1 C_2}{C_1 + C_2}\right)} \tag{150}$$

rather than simply $1/\omega C_2$. The actual corner frequencies may in general also be slightly displaced from the values shown. For this example, the pole frequencies f_1 and f_2 given above are the exact values, while the exact zero frequency f_3 is 1096 Hz rather than 965 Hz.

When adding asymptotes having the same slopes, such as R_1 and R_2 in this example, the actual asymptote is the sum $(R_1 + R_2)$ rather than simply the largest. Likewise, the parallel combination of two asymptotes having the same slope is actually given by the inverse addition formula, rather than simply the smaller asymptote. So the "algebra on the graph" method is an approximation. The worst case, having least accuracy, occurs when the asymptotes having the same slope also have the same magnitude —the approximate asymptote will then differ by 6dB. When the two impedances have different values, then the deviation will be less than 6dB. Also implicit in the "algebra on the graph" method is the approximate factorization of the numerator and denominator polynomials of the impedance or transfer function. The accuracy of the result is high when the corner frequencies are well separated in magnitude.

The fact that the graphical construction method yields an approximate answer should not be viewed as a disadvantage. Indeed, this is a great advantage of the method: Bode diagrams of reasonable accuracy can be obtained very quickly. Much physical understanding of the circuit can be gained, because simple analytical expressions are found

for how the salient features (corner frequencies and asymptote values) depend on the component values. Suitable approximations become obvious.

In the majority of design situations, absolute accuracy is not so important. Instead, it is more important for the design engineer to gain insight into how the circuit works, so that he or she can figure out how to make the circuit behave as desired. Simple approximations are the key to obtaining this insight; more exact (and more complicated) equations may remain as enigmatic as the original circuit. In those cases where more accuracy is needed, and where it is judged worthwhile to expend the effort, a less approximate analysis can still be performed.

The graphical construction method for impedance magnitudes is well known, and "impedance graph" paper can be purchased commercially. As illustrated in Fig. 41, the magnitudes of the impedances of various inductances, capacitances, and resistances are plotted on semilogarithmic axes. Asymptotes for the impedances of *R*-*L*-*C* networks can be sketched directly on these axes, and numerical values of corner frequencies can then be graphically determined.

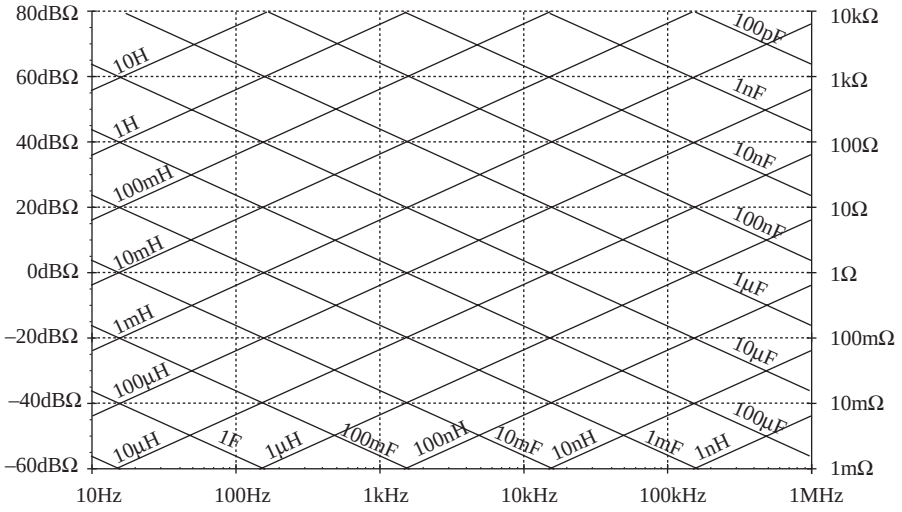

Fig. 41. "Impedance graph": an aid for graphical construction of impedances, with the magnitudes of various inductive, capacitive, and resistive impedances pre-plotted.

3.4. Voltage divider transfer functions: division of asymptotes

Usually, we can express transfer functions in terms of impedances —for example, as the ratio of two impedances. If we can construct these impedances as described in the previous section, then we can also construct the transfer function $H_e(s)$ of a single-section two-pole filter example, Fig. 42, is constructed using the voltage divider formula.

The familiar voltage divider formula shows that the transfer function of this circuit can be expressed as the ratio of impedances Z_2 / Z_{in}, where $Z_{in} = Z_1 + Z_2$ is the network input impedance:

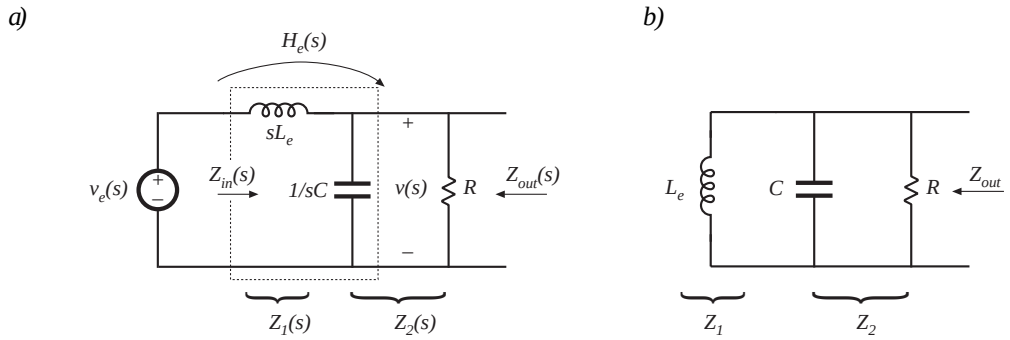

Fig. 42. Transfer function $H_e(s)$ and output impedance $Z_{out}(s)$ of a single-section L-C filter: (a) circuit, with H_e and Z_{out} identified; (b) determination of Z_{out}, by setting independent sources to zero.

$$\frac{\hat{v}(s)}{\hat{v}_e(s)} = \frac{Z_2}{Z_1+Z_2} = \frac{Z_2}{Z_{in}} \tag{151}$$

For the example of Fig. 42, $Z_1(s) = sL_e$, and $Z_2(s)$ is the parallel combination of R and $1/sC$. Hence, we can find the transfer function asymptotes by constructing the asymptotes of Z_2 and of the series combination represented by Z_{in}, and then dividing. Another approach, which is easier to apply in this example, is to multiply the numerator and denominator of Eq. (151) by Z_1:

$$\frac{\hat{v}(s)}{\hat{v}_e(s)} = \frac{Z_2 Z_1}{Z_1+Z_2}\,\frac{1}{Z_1} = \frac{Z_{out}}{Z_1} \tag{152}$$

where $Z_{out} = Z_1 \parallel Z_2$ is the output impedance of the voltage divider. So another way to construct the voltage divider transfer function is to first construct the asymptotes for Z_1 and for the parallel combination represented by Z_{out}, and then divide. This method is useful when the parallel combination $Z_1 \parallel Z_2$ is easier to construct than the series combination $Z_1 + Z_2$. It often gives a different approximate result, which may be more (or sometimes less) accurate than the result obtained using Z_{in}.

The output impedance Z_{out} in Fig. 42(b) is

$$Z_{out}(s) = R \parallel \frac{1}{sC} \parallel sL_e \tag{153}$$

The impedance of the parallel R-L-C network is constructed in section 3.2, and is illustrated in Fig. 43(a) for the high-Q case.

According to Eq. (152), the voltage divider transfer function magnitude is $|| H_e ||$ = $|| Z_{out} ||$ / $|| Z_1 ||$. This quantity is constructed in Fig. 43(b). For $\omega < \omega_0$, the asymptote of $|| Z_{out} ||$ coincides with $|| Z_1 ||$: both are equal to ωL_e. Hence, the ratio is $|| Z_{out} ||$ / $|| Z_1 ||$ = 1. For $\omega > \omega_0$, the asymptote of $|| Z_{out} ||$ is $1/\omega C$, while $|| Z_1 ||$ is equal to ωL_e. The ratio then becomes $|| Z_{out} ||$ / $|| Z_1 ||$ = $1/\omega^2 L_e C$, and hence the high-frequency asymptote has a –40dB/decade slope. At $\omega = \omega_0$, $|| Z_{out} ||$ has exact value R, while $|| Z_1 ||$ has

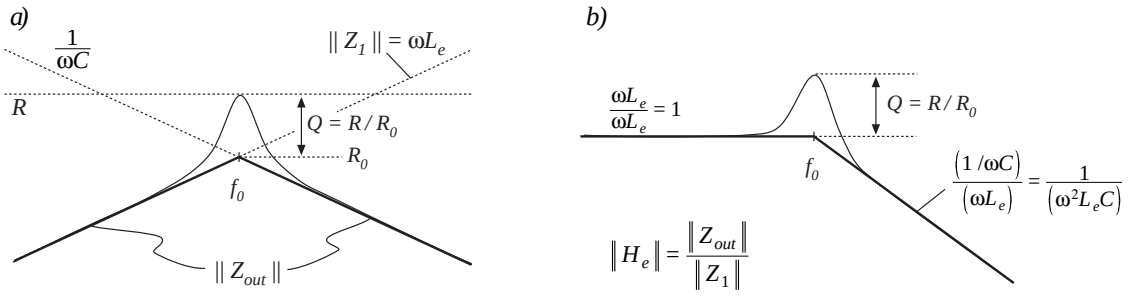

Fig. 43. Graphical construction of H_e and Z_{out}: (a) output impedance Z_{out}; (b) transfer function H_e.

exact value R_0. The ratio is then $\| H_e(j\omega_0) \| = \| Z_{out}(j\omega_0) \| / \| Z_1(j\omega_0) \| = R / R_0 = Q$. So the filter transfer function H_e has the same ω_0 and Q as the impedance Z_{out}.

It now becomes obvious how variations in element values affect the salient features of the transfer function and output impedance. For example, the effect of increasing the inductance value L_e on the output impedance is illustrated in Fig. 44. It can be seen that increasing L_e causes the angular resonant frequency ω_0 to be reduced, and also reduces the Q-factor.

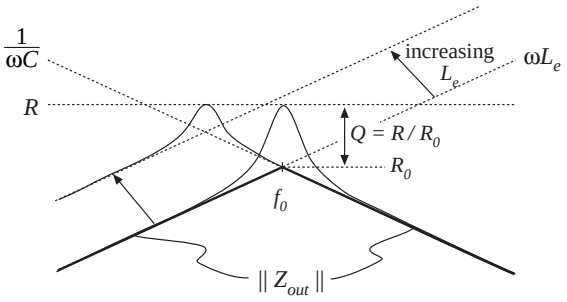

Fig. 44. Variation of output impedance asymptotes, corner frequency, and Q-factor with increasing inductance L_e.

4. Measurement of ac transfer functions and impedances

It is good engineering practice to measure the transfer functions of prototype systems. Such an exercise can verify that the system has been correctly modeled and designed. Also, it is often useful to characterize individual circuit elements through measurement of their terminal impedances.

Small-signal ac magnitude and phase measurements can be made using an instrument known as a *network analyzer*, or *frequency response analyzer*. The key inputs and outputs of a basic network analyzer are illustrated in Fig. 45.

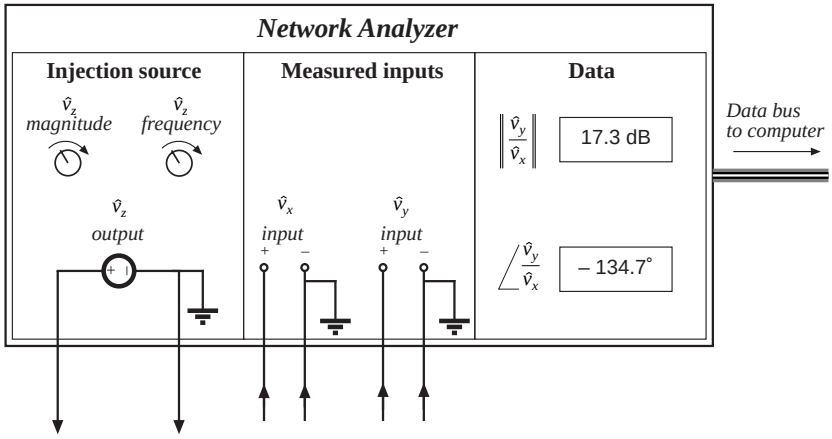

Fig.45. Key features and functions of a network analyzer: sinusoidal source of controllable amplitude and frequency, two analog inputs, and determination of relative magnitude and phase of the input components at the injection frequency.

The network analyzer provides a sinusoidal output voltage $\hat{v}_z$ of controllable amplitude and frequency. This signal can be injected into the system to be measured, at any desired location. The network analyzer also has two (or more) inputs, $\hat{v}_x$ and $\hat{v}_y$. The return electrodes of $\hat{v}_z$, $\hat{v}_x$ and $\hat{v}_y$ are internally connected to earth ground. The network analyzer performs the function of a narrowband tracking voltmeter: it measures the components of $\hat{v}_x$ and $\hat{v}_y$ at the injection frequency, and displays the magnitude and phase of the quantity $\hat{v}_y / \hat{v}_x$. The narrowband tracking voltmeter feature is essential for measurements over a wide range of magnitudes; otherwise, noise and interference from neighboring circuits corrupt the desired sinusoidal signals and make accurate measurements impossible [3]. Modern network analyzers can automatically sweep the frequency of the injection source $\hat{v}_z$ to generate magnitude and phase Bode plots of the transfer function $\hat{v}_y / \hat{v}_x$.

A typical test setup for measuring the transfer function of an amplifier is illustrated in Fig. 46. A potentiometer, connected between a dc supply voltage V_{CC} and ground, is used to bias the amplifier input to attain the correct quiescent operating point. The injection source voltage $\hat{v}_z$ is coupled to the amplifier input terminals via a dc blocking capacitor. This blocking capacitor prevents the injection voltage source from upsetting the dc bias. The network analyzer inputs $\hat{v}_x$ and $\hat{v}_y$ are connected to the input and output terminals of the amplifier. Hence, the measured transfer function is

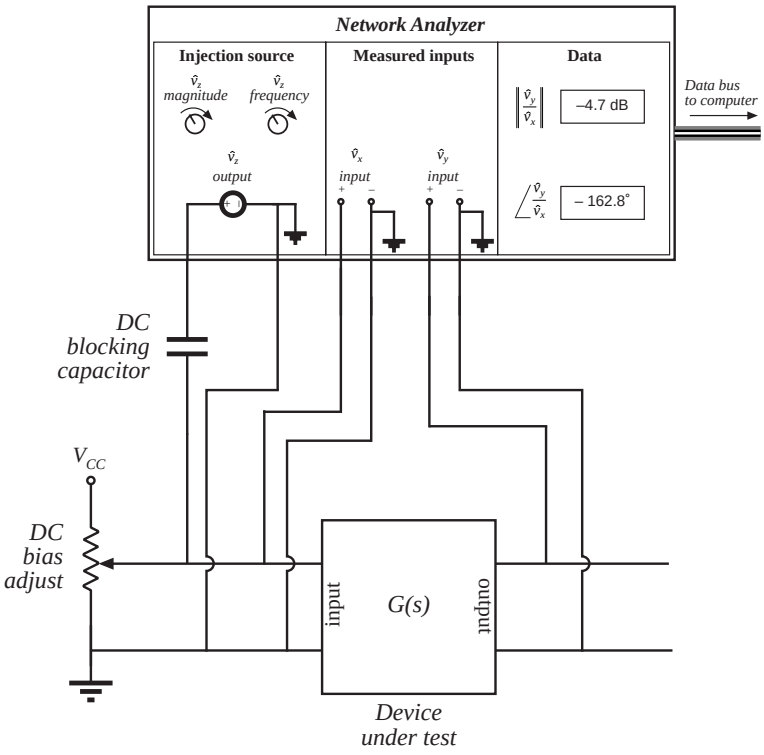

Fig. 46. Measurement of a transfer function.

$$\frac{\hat{v}_y(s)}{\hat{v}_x(s)} = G(s) \tag{154}$$

Note that the blocking capacitance, bias potentiometer, and $\hat{v}_z$ amplitude have no effect on the measured transfer function.

An impedance

$$Z(s) = \frac{\hat{v}(s)}{\hat{i}(s)} \tag{155}$$

can be measured by treating the impedance as a transfer function from current to voltage. For example, measurement of the output impedance of an amplifier is illustrated in Fig. 47. The quiescent operating condition is again established by a potentiometer which biases the amplifier input. The injection source $\hat{v}_z$ is coupled to the amplifier output through a dc blocking capacitor. The injection source voltage $\hat{v}_z$ excites a current $\hat{i}_{out}$ in impedance Z_s. This current flows into the output of the amplifier, and excites a voltage across the amplifier output impedance:

$$Z_{out}(s) = \left. \frac{\hat{v}_y(s)}{\hat{i}_{out}(s)} \right|_{\substack{amplifier \\ ac\ input = 0}} \tag{156}$$

A current probe is used to measure $\hat{i}_{out}$. The current probe produces a voltage proportional to $\hat{i}_{out}$; this voltage is connected to the network analyzer input $\hat{v}_x$. A voltage probe is used to measure the amplifier output voltage $\hat{v}_y$. The network analyzer displays the transfer function $\hat{v}_y / \hat{v}_x$, which is proportional to Z_{out}. Note that the value of Z_s and the amplitude of $\hat{v}_z$ do not affect the measurement of Z_{out}.

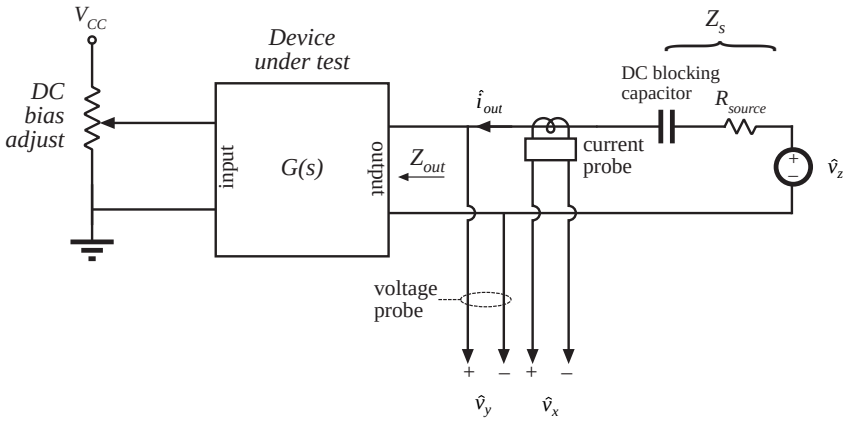

Fig. 47. Measurement of the output impedance of a system.

It is sometimes necessary to measure impedances that are very small in magnitude. Grounding problems cause the test setup of Fig. 47 to fail in such cases. The reason is illustrated in Fig. 48(a). Since the return connections of the injection source $\hat{v}_z$ and the analyzer input $\hat{v}_y$ are both connected to earth ground, the injected current $\hat{i}_{out}$ can return to the source through the return connections of either the injection source or the voltage probe. In practice, $\hat{i}_{out}$ divides between the two paths according to their relative impedances. Hence, a significant current $(1 - k)\ \hat{i}_{out}$ flows through the return connection of the voltage probe. If the voltage probe return connection has some total contact and wiring impedance Z_{probe}, then the current induces a voltage drop $(1 - k)\ \hat{i}_{out}\ Z_{probe}$ in the voltage probe wiring, as illustrated in Fig. 48(a). Hence, the network analyzer does not correctly measure the

a)

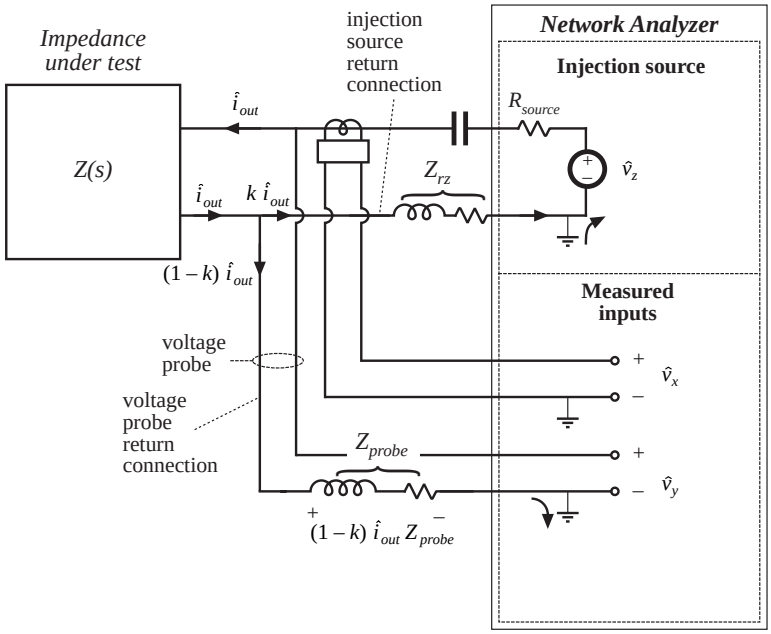

b)

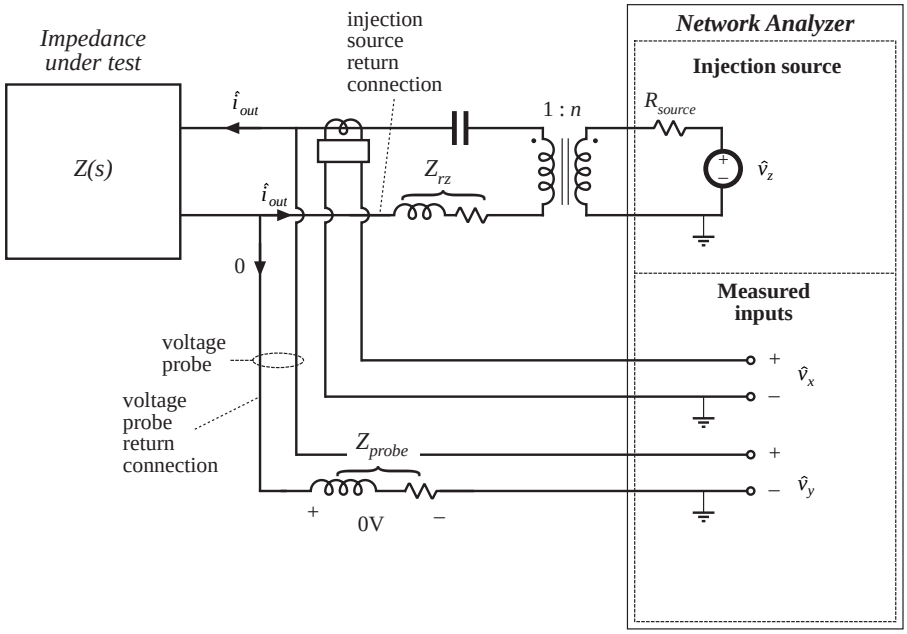

Fig. 48. Measurement of a small impedance *Z(s)*: (a) current flowing in the return connection of the voltage probe induces a voltage drop which corrupts the measurement; (b) an improved experiment, incorporating isolation of the injection source.

voltage drop across the impedance *Z*. If the internal ground connections of the network analyzer have negligible impedance, then the network analyzer will display the following impedance:

$$Z + (1-k)\,Z_{probe} = Z + Z_{probe} \,||\, Z_{rz} \tag{157}$$

Here, Z_{rz} is the impedance of the injection source return connection. So to obtain an accurate measurement, the following condition must be satisfied:

$$\| Z \| >> \left\| \left(Z_{probe} \| Z_{rz} \right) \right\| \tag{158}$$

A typical lower limit on $\| Z \|$ is a few tens or hundreds of milliohms.

An improved test setup for measurement of small impedances is illustrated in Fig. 48(b). An isolation transformer is inserted between the injection source and the dc blocking capacitor. The return connections of the voltage probe and injection source are no longer in parallel, and the injected current $\hat{i}_{out}$ must now return entirely through the injection source return connection. An added benefit is that the transformer turns ratio n can be increased, to better match the injection source impedance to the impedance under test. Note that the impedances of the transformer, of the blocking capacitor, and of the probe and injection source return connections, do not affect the measurement. Much smaller impedances can therefore be measured using this improved approach.

5. Summary of key points

1. The magnitude Bode diagrams of functions which vary as $(f / f_0)^n$ have slopes equal to $20n$ dB per decade, and pass through 0dB at $f = f_0$.
2. It is good practice to express transfer functions in normalized pole-zero form; this form directly exposes expressions for the salient features of the response, i.e., the corner frequencies, reference gain, etc.
3. Poles and zeroes can be expressed in frequency-inverted form, when it is desirable to refer the gain to a high-frequency asymptote.
4. A two-pole response can be written in the standard normalized form of Eq. (50). When $Q > 0.5$, the poles are complex conjugates. The magnitude response then exhibits peaking in the vicinity of the corner frequency, with an exact value of Q at $f = f_0$. High Q also causes the phase to change sharply near the corner frequency.
5. When the Q is less than 0.5, the two pole response can be plotted as two real poles. The low-Q approximation predicts that the two poles occur at frequencies f_0 / Q and Qf_o. These frequencies are within 10% of the exact values for $Q \leq 0.3$.
6. The low-Q approximation can be extended to find approximate roots of an arbitrary degree polynomial. Approximate analytical expressions for the salient features can be derived. Numerical values are used to justify the approximations.
7. Approximate magnitude asymptotes of impedances and transfer functions can be easily derived by graphical construction. This approach is a useful supplement to conventional analysis, because it yields physical insight into the circuit behavior,

and because it exposes suitable approximations. Several examples, including the impedances of basic series and parallel resonant circuits and the transfer function $H_e(s)$ of a single-section filter circuit, are worked in section 3.

8. Measurement of transfer functions and impedances using a network analyzer is discussed in section 4. Careful attention to ground connections is important when measuring small impedances.

REFERENCES

[1] R.D. Middlebrook, "Low Entropy Expressions: The Key to Design-Oriented Analysis," *IEEE Frontiers in Education Conference*, 1991 Proceedings, pp. 399-403, Sept. 1991.

[2] R. D. Middlebrook, "Methods of Design-Oriented Analysis: The Quadratic Equation Revisited," *IEEE Frontiers in Education Conference*, 1992 Proceedings, pp. 95-102, Nov. 1991.

[3] F. Barzegar, S. Cuk, and R. D. Middlebrook, "Using Small Computers to Model and Measure Magnitude and Phase of Regulator Transfer Functions and Loop Gain," *Proceedings of Powercon 8*, April 1981. Also in *Advances in Switched-Mode Power Conversion*, Irvine: Teslaco, vol. 1, pp. 251-278, 1981.

PROBLEMS

1 . Express the gains represented by the asymptotes of Figs. 49(a)-(c) in factored pole-zero form. You may assume that all poles and zeroes have negative real parts.

2 . Derive analytical expressions for the low-frequency asymptotes of the magnitude Bode plots shown in Fig. 50(a)-(c).

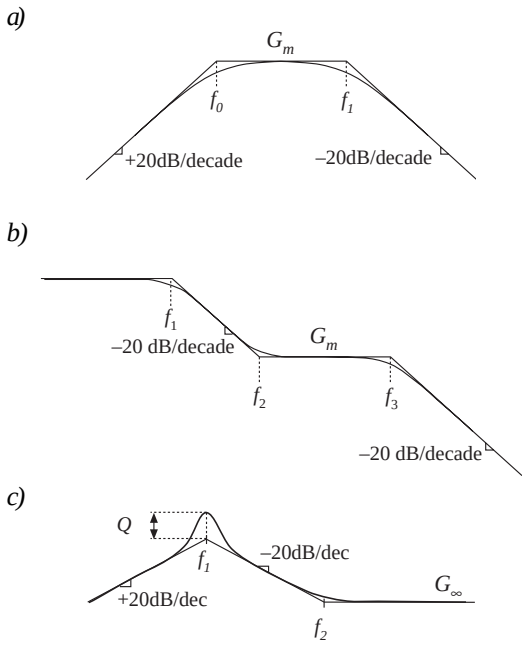

Fig. 49.

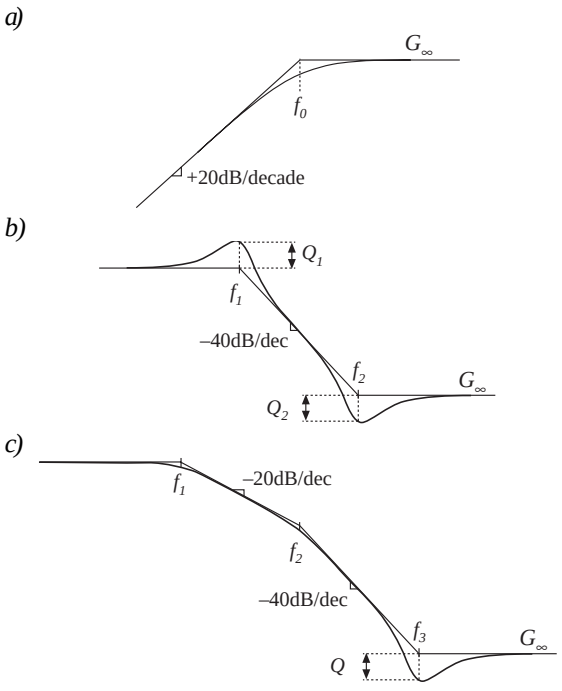

Fig. 50.

3 . Express the gains represented by the asymptotes of Figs. 50(a)-(c) in factored pole-zero form. You may assume that all poles and zeroes have negative real parts.

4 . Derive analytical expressions for the three magnitude asymptotes of Fig. 14.

5 . An experimentally-measured transfer function. Figure 51 contains experimentally-measured magnitude and phase data for the gain function *A(s)* of a certain amplifier. The object of this problem is to find an expression for *A(s)*. Overlay asymptotes as appropriate on the magnitude and phase data, and hence deduce numerical values for the gain asymptotes and corner frequencies of *A(s)*. Your magnitude and phase asymptotes must, of course, follow all of the rules: magnitude slopes must be multiples of ±20dB/decade, phase slopes for real poles must be multiples of ±45˚/decade, etc. The phase and magnitude asymptotes must be consistent with each other.

It is suggested that you start by guessing *A(s)* based on the magnitude data. Then construct the phase asymptotes for your guess, and compare them with the given data. If there are discrepancies, then modify your guess accordingly and re-do your magnitude and phase asymptotes. You should

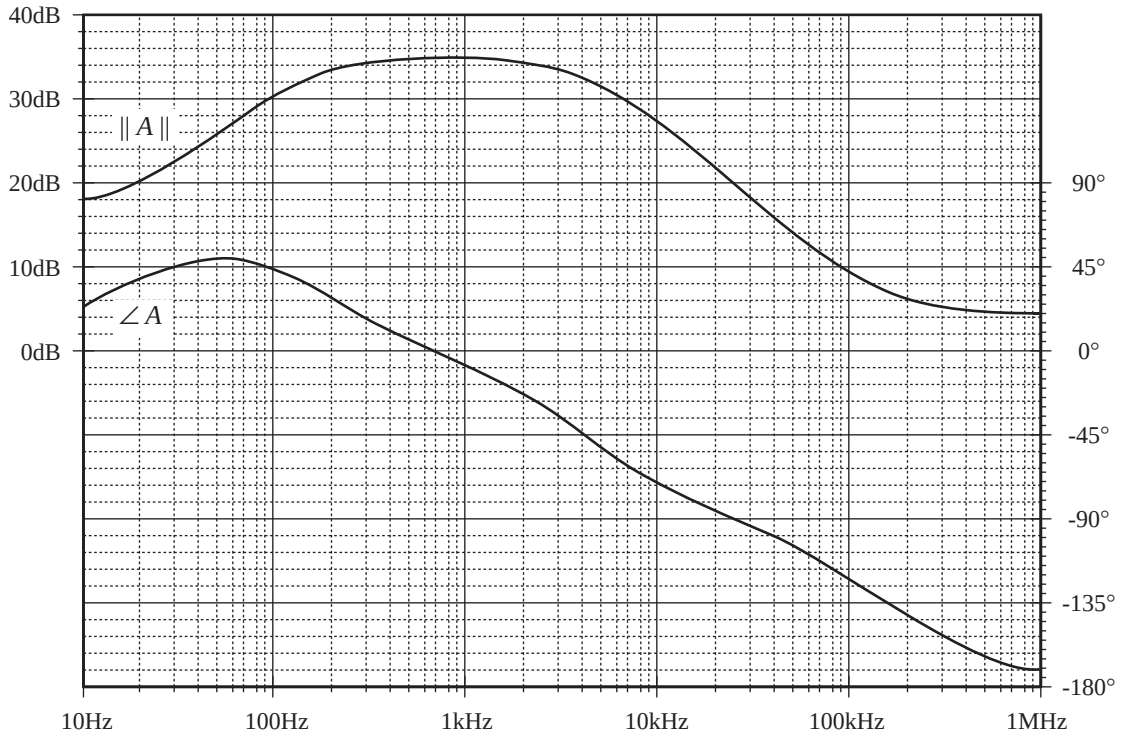

Fig. 51.

turn in: (1) your analytical expression for *A(s)*, with numerical values given, and (2) a copy of Fig. 51, with your magnitude and phase asymptotes superimposed and with all break frequencies and slopes clearly labeled.

6 . An experimentally-measured impedance. Figure 52 contains experimentally-measured magnitude and phase data for the driving-point impedance *Z(s)* of a passive network. The object of this problem is the find an expression for *Z(s)*. Overlay asymptotes as appropriate on the magnitude and phase data, and hence deduce numerical values for the salient features of the impedance function. You should turn in: (1) your analytical expression for *Z(s)*, with numerical values given,

and (2) a copy of Fig. 52, with your magnitude and phase asymptotes superimposed and with all salient features and asymptote slopes clearly labeled.

7. Magnitude Bode diagram of an R-L-C filter circuit. For the filter circuit of Fig. 53, construct the Bode plots for the magnitudes of the Thevenin-equivalent output impedance Z_{out} and the transfer function $H(s) = v_2 / v_1$. Plot your results on semi-log graph paper. Give approximate analytical expressions and numerical values for the important corner frequencies and asymptotes. Do all of the elements significantly affect Z_{out} and H?

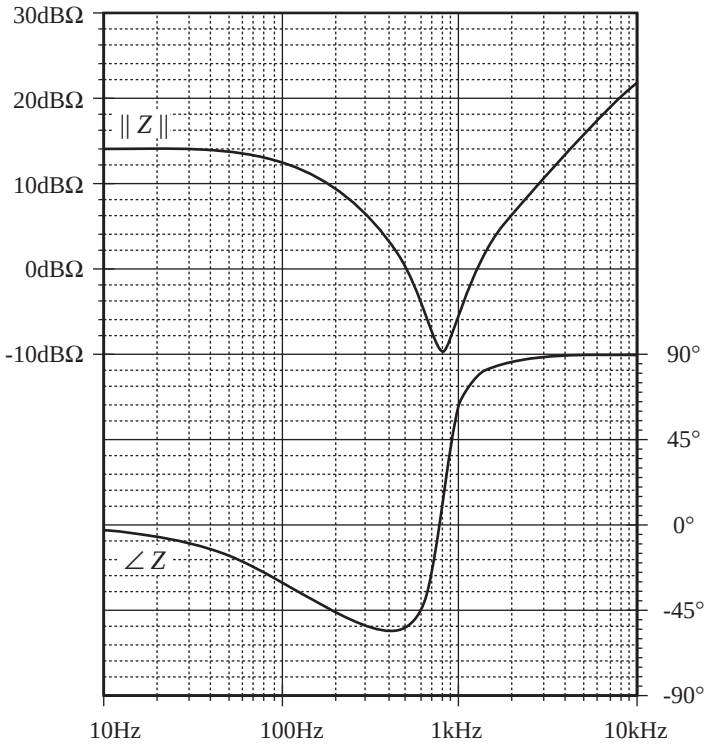

Fig. 52.

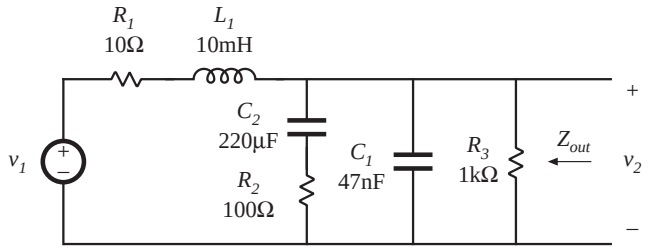

Fig. 53.

8. Operational amplifier filter circuit. The op amp circuit shown in Fig. 54 is a practical realization of what is known as a PID controller, and is sometimes used to modify the loop gain of feedback circuits to improve their performance. Using semilog graph paper, sketch the Bode diagram of the magnitude of the transfer function $v_2(s) / v_1(s)$ of the circuit shown. Label all corner frequencies, flat asymptote gains, and asymptote slopes, as appropriate, giving both analytical expressions and numerical values. You may assume that the op amp is ideal.

9. Phase asymptotes. Construct the phase asymptotes for the transfer function $v_2(s) / v_1(s)$ of problem 8. Label all break frequencies, flat asymptotes, and asymptote slopes.

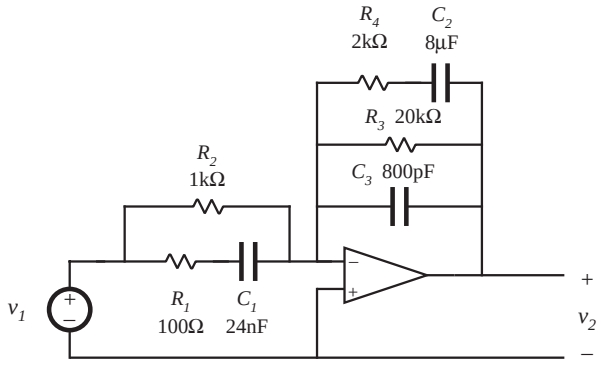

Fig. 54.

10. Construct the Bode diagram for the magnitude of the output impedance Z_{out} of the network shown in Fig. 55. Give suitable analytical expressions for each asymptote, corner frequency, and Q-factor, as appropriate. Justify any approximations that you use.

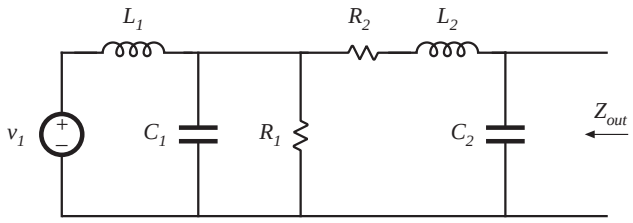

Fig. 55.

The component values are:

L_1 = 100μH L_2 = 16mH

C_1 = 1000μF C_2 = 10μF

R_1 = 5Ω R_2 = 50Ω

11. The two section filter in the circuit of Fig. 56 should be designed such that its output impedance $Z_s|_{v_g} = 0$ meets certain filter design criteria, and hence it is desirable to construct the Bode plot for the magnitude of Z_s. Although this filter contains six reactive elements, $\| Z_s \|$ can nonetheless be constructed in a relatively straightforward manner using graphical construction techniques. The element values are:

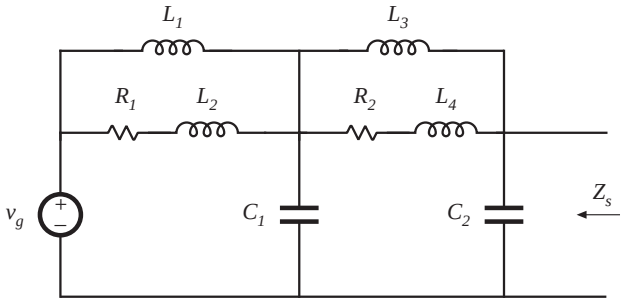

Fig. 56.

L_1 = 32mH C_1 = 32μF

L_2 = 400μH C_2 = 6.8μF

L_3 = 800μH R_1 = 10Ω

L_4 = 1μH R_2 = 1Ω

(a) Construct $\| Z_s \|$ using the "algebra on the graph" method. Give simple approximate analytical expressions for all asymptotes and corner frequencies.

(b) It is desired that $\| Z_s \|$ be approximately equal to 5Ω at 500Hz and 2.5Ω at 1kHz. Suggest a simple way to accomplish this by changing the value of one component.

12. A two-section L-C filter has the following transfer function:

$$G(s) = \frac{1}{1 + s\left(\frac{L_1 + L_2}{R}\right) + s^2\left(L_1\left(C_1 + C_2\right) + L_2C_2\right) + s^3\left(\frac{L_1L_2C_1}{R}\right) + s^4\left(L_1L_2C_1C_2\right)}$$

The element values are:

R	50mΩ		
C_1	680μF	C_2	4.7μF
L_1	500μH	L_2	50μH

(a) Factor *G(s)* into approximate real and quadratic poles, as appropriate. Give analytical expressions for the salient features. Justify your approximation using the numerical element values.

(b) Construct the magnitude and phase asymptotes of *G(s)*.

(c) It is desired to reduce the *Q* to 2, without significantly changing the corner frequencies or other features of the response. It is possible to do this by changing only two element values. Specify how to accomplish this.

13. Output impedance of a two-section input filter. Construct the asymptotes for the magnitude of the output impedance, $\| Z_{out} \|$ of the damped two-section input filter shown in Fig. 57. You may use suitable approximations. Label all corner frequencies, asymptotes, and any Q-factors, with approximate analytical expressions. No credit will be given for computer-generated plots. The component values are:

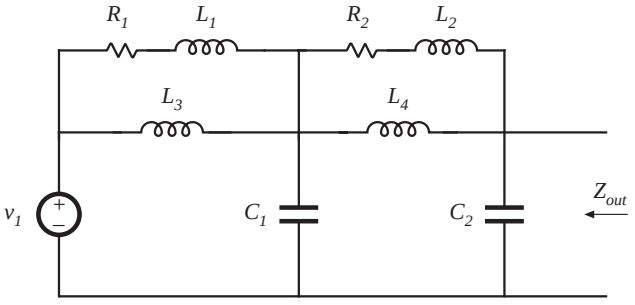

Fig. 57.

R_1	2Ω	R_2	10Ω
C_1	10μF	C_2	1μF
L_1	32μH	L_2	8μH
L_3	3.2mH	L_4	320μH

14. A resonant *LCC* circuit contains the following transfer function:

$$H(s) = \frac{sC_1R}{1 + sR(C_1 + C_2) + s^2LC_1 + s^3LC_1C_2R}$$

(a) When C_1 is sufficiently large, this transfer function can be expressed as an inverted pole and a quadratic pole pair. Derive analytical expressions for the corner frequencies and *Q*-factor in this case, and sketch typical magnitude asymptotes. Determine analytical conditions for validity of your approximation.

(b) When C_2 is sufficiently large, the transfer function can be also expressed as an inverted pole and a quadratic pole pair. Derive analytical expressions for the corner frequencies and *Q*-factor in this case, and sketch typical magnitude asymptotes. Determine analytical conditions for validity of your approximation in this case.

(c) When $C_1 = C_2$ and when the quadratic poles have sufficiently high *Q*, then the transfer function can again be expressed as an inverted pole and a quadratic pole pair. Derive analytical expressions for the corner frequencies and *Q*-factor in this case, and sketch typical magnitude asymptotes. Determine analytical conditions for validity of your approximation in this case.